Supporting Information

Synthesis of Fully-Fused Bisboron Azomethine Complexes and Their Conjugated Polymers with Solid-State Near-Infrared Emission

Shunsuke Ohtani, Masashi Nakamura, Masayuki Gon, Kazuo Tanaka* and Yoshiki Chujo

Department of Polymer Chemistry, Graduate School of Engineering, Kyoto University Katsura, Nishikyo-ku, Kyoto 615-8510, Japan

E-mail: tanaka@poly.synchem.kyoto-u.ac.jp

Contents:

General

^{1}H (400 MHz), ^{13}C (100 MHz) ^{11}B (128 MHz) NMR spectra were recorded on JEOL JNM-AL400 or JNM-EX400 spectrometers. Samples were analyzed in $CDCl_3$ and CD_2Cl_2. The chemical shift values were expressed relative to tetramethylsilane (TMS) for ^{1}H and ^{13}C NMR as an internal standard in $CDCl_3$ and $BF_3{\cdot}OEt_2$ for ^{11}B NMR as a capillary standard. Analytical thin-layer chromatography (TLC) was performed with silica gel 60 Merck F254 plates. Column chromatography was performed with Wakogel® C-300 silica gel. High-resolution mass (HRMS) spectrometry was performed at the Technical Support Office (Department of Synthetic Chemistry and Biological Chemistry, Graduate School of Engineering, Kyoto University), and the HRMS spectra were obtained on a Thermo Fisher Scientific EXACTIVE spectrometer for electrospray ionization (ESI) and a JEOL EXACTIVE spectrometer for Electron Ionizaion (EI) and a Bruker Daltonics ultrafleXtreme for Matrix Assisted Laser Desorption ionization (MALDI). UV–vis–NIR absorption spectra were recorded on a SHIMADZU UV-3600 spectrophotometer, and samples were analyzed at room temperature. Photoluminescence (PL) spectra in solution state were measured on a HORIBA Fluorolog-3 luminescence spectrometer and samples were analyzed at room temperature. Photoluminescence (PL) spectra were measured on a HORIBA Fluorolog-3 luminescence spectrometer and an Ocean Optics USB4000 for solution samples using a white diode laser (LLS-Cool-White), and samples were analyzed at room temperature. Absolute PL quantum efficiency was measured on a Hamamatsu Photonics Quantaurus-QY Plus C13534-01. Cyclic voltammetry (CV) was carried out on a BASALS-Electrochemical-Analyzer Model 600D with a glassy carbon working electrode, a Pt counter electrode, an Ag/AgCl reference electrode, and the ferrocene/ferrocenium (Fc/Fc^{+}) external reference at a scan rate of 0.1 Vs^{-1}. The PL lifetime measurement was performed on a Horiba FluoroCube spectrofluorometer system; excitation was carried out using a UV diode laser (NanoLED 290 nm and 375 nm). X-ray crystallographic analysis was carried out by Rigaku R-AXIS RAPID-F graphite-monochromated MoKα radiation diffractometer with an imaging plate. A symmetry-related absorption correction was carried out by using the program ABSCOR. The analysis was carried out with direct methods (SHELX-97) using Yadokari-XG. The program Mercury 3.3.1 was used to generate the X-ray structural diagram.

Materials

<u>Commercially available compounds used without purification:</u>

Magnesium (Turnings) (Wako Pure Chemical Industries, Ltd.)

Iodine (Wako Pure Chemical Industries, Ltd.)

Bromobenzene (Wako Pure Chemical Industries, Ltd.)

Methyl anthranilate (Tokyo Chemical Industry Co, Ltd.)

2,5-Dimethoxybenzene-1,4-dicarboxaldehyde (Sigma-Aldrich Co. LLC.)

Boron tribromide (17% in CH_2Cl_2, ca. 1 M) (BBr_3 in CH_2Cl_2) (Tokyo Chemical Industry Co, Ltd.)

Salicylaldehyde (Tokyo Chemical Industry Co, Ltd.)

Phenylboronic acid (Wako Pure Chemical Industries, Ltd.)

Methyl 5-bromo anthranilate (Tokyo Chemical Industry Co, Ltd.)

Dichlorophenylborane (Tokyo Chemical Industry Co, Ltd.)

Commercially available solvents:

MeCN (Wako Pure Chemical Industries, Ltd.), EtOH (Wako Pure Chemical Industries, Ltd.), $CHCl_3$ (Wako Pure Chemical Industries, Ltd.), hexane (Wako Pure Chemical Industries, Ltd.), EtOAc (Wako Pure Chemical Industries, Ltd.), CH_2Cl_2 (Wako Pure Chemical Industries, Ltd.), CH_2Cl_2 (deoxidized grade, Wako Pure Chemical Industries, Ltd.) and toluene (deoxidized grade, Wako Pure Chemical Industries, Ltd.) were used without further purification. THF (Kanto Chemical Co., Inc.) and Et_2O (Kanto Chemical Co., Inc.) were purified by passage through solvent purification columns under argon pressure.

Compounds prepared as described in the literatures:

2,5-Dihydroxybenzene-1,4-dicarboxaldehyde **(2)**[1]

Synthetic Procedures and Characterization

Synthesis of 1

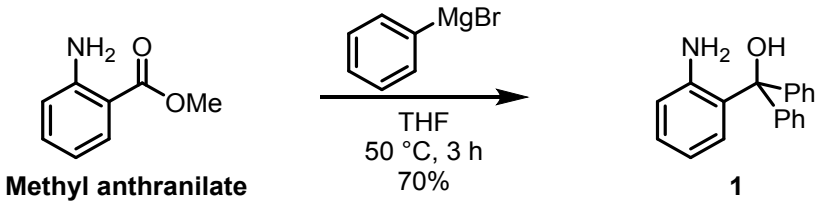

Scheme S1. Synthesis of compound **1**.

Phenylmagnesium bromide (1.0 M in THF) was prepared prior to use. Mg (1.27 g, 53.0 mmol) in dry THF was activated with I_2 under argon atmosphere. Phenyl bromide (4.2 mL, 39.7 mmol) in dry THF (40 mL) was added slowly into the solution. After addition was complete, the mixture was stirred at room temperature for 1 h. To a solution of methyl anthranilate (2.0 g, 13.2 mmol) in THF (13 mL) was added slowly into 1.0 M phenylmagnesium bromide in THF (40 mL) at 0 °C. The mixture was heated to 50 °C and stirred for 3 h. After cooling to room temperature, the mixture was quenched by 1.0 M HCl aqueous solution. Then, the product was extracted with EtOAc. Organic layers were washed with brine, dried over $MgSO_4$ and evaporated to afford a brown solid. The solid was purified by column chromatography on SiO_2 (hexane/EtOAc = 3/1 v/v as an eluent) and further purification was carried out by recrystallization from hexane to afford **1** (0.571 g, 2.36 mmol, 24%) as a light brown powder.

R_f = 0.45 (hexane/EtOAc = 3/1 v/v). ^{1}H NMR (CD_2Cl_2, 400 MHz), δ (ppm): 7.36–7.27 (m, 10H), 7.14 (td, J = 7.5, 1.5 Hz, 1H), 6.80 (dd, J = 7.9, 1.1 Hz, 1H), 6.70 (td, J = 7.5, 1.1 Hz, 1H), 6.48 (dd, J = 7.9, 1.4 Hz, 1H), 4.50 (bs, 2H). ^{13}C NMR (CD_2Cl_2, 100 MHz), δ (ppm): 146.2, 144.5, 133.5, 130.1, 129.1, 128.5, 128.2, 128.1, 127.7, 119.4, 82.7. HRMS (ESI): Calcd for $[M+Na]^+$, 298.1202; found, m/z 298.1205.

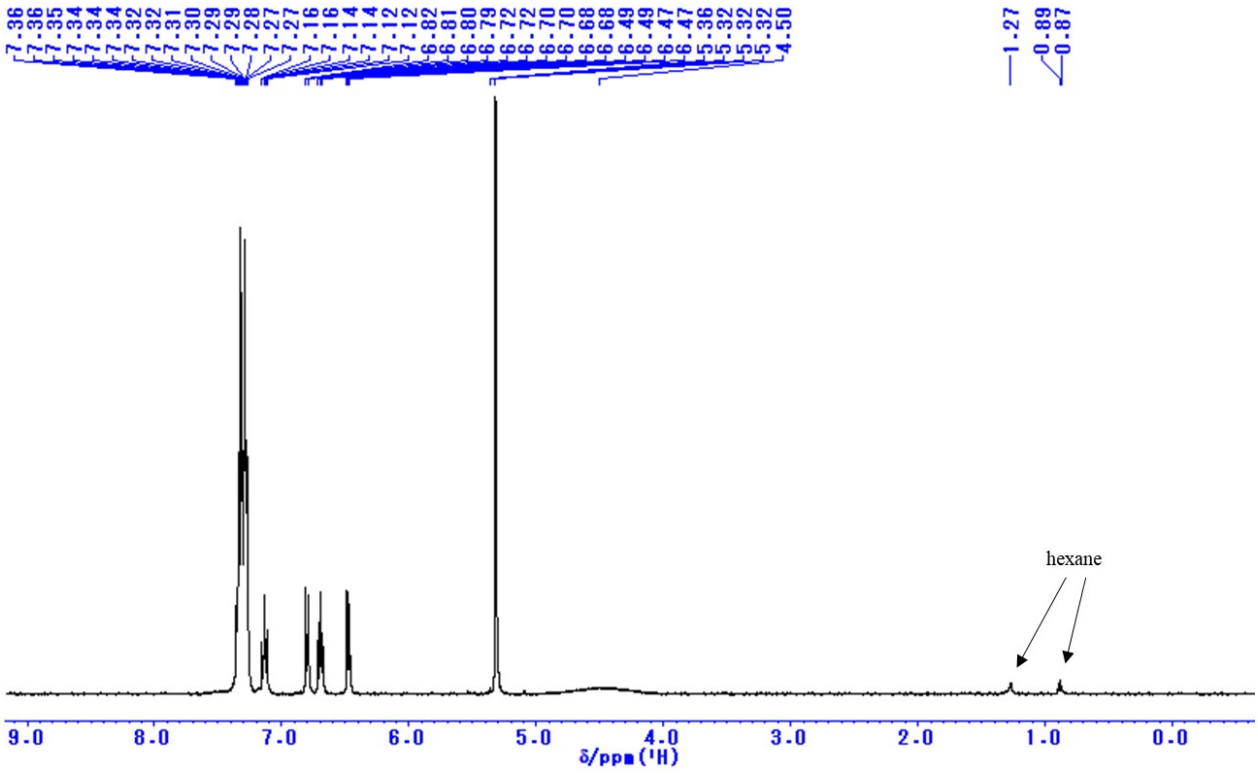

Fig. S1. ^{1}H NMR spectrum of **1**, CD_2Cl_2, 400 MHz.

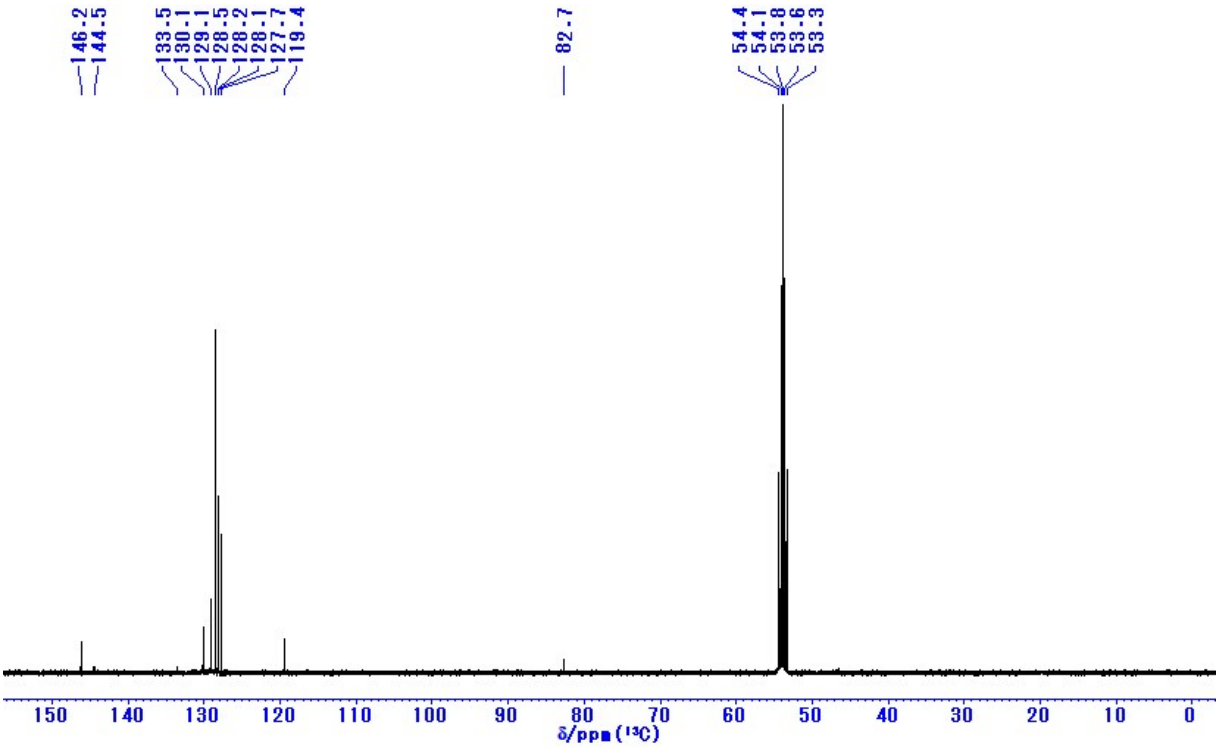

Fig. S2. ^{13}C NMR spectrum of **1**, $CDCl_3$, 100 MHz.

Synthesis of 2

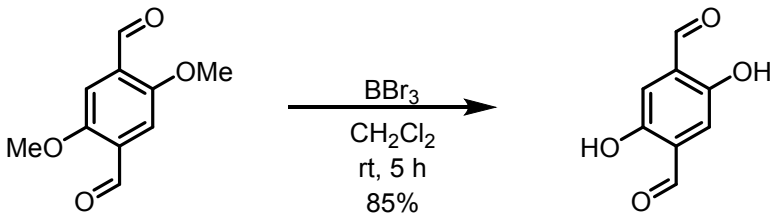

2,5-Dimethoxybenzene-1,4-dicarboxaldehyde **2**

Scheme S2. Synthesis of compound **2**.

2,5-Dimethoxybenzene-1,4-dicarboxaldehyde (1.00 g, 2.48 mmol) was dissolved in dry CH_2Cl_2 (21 mL) under argon atmosphere at room temperature and BBr_3 (20.6 mL, 20.6 mmol) was then added to the reaction mixture at −78 °C. After stirring for 5 h at room temperature, the reaction mixture was quenched by EtOH at 0 °C. The resulting mixture was filtered and dried *in vacuo* at 80 °C to afford **2** as a yellow solid (0.73 g, 85%). The analytical spectral data of ^{1}H NMR were identical with literature references.(6)

^{1}H NMR ($CDCl_3$, 400 MHz), δ (ppm): 10.2 (s, 2H), 9.96 (s, 2H), 7.24 (s, 2H). HRMS (EI): Calcd for $[M]^+$, 166.0266; found, m/z 166.0263.

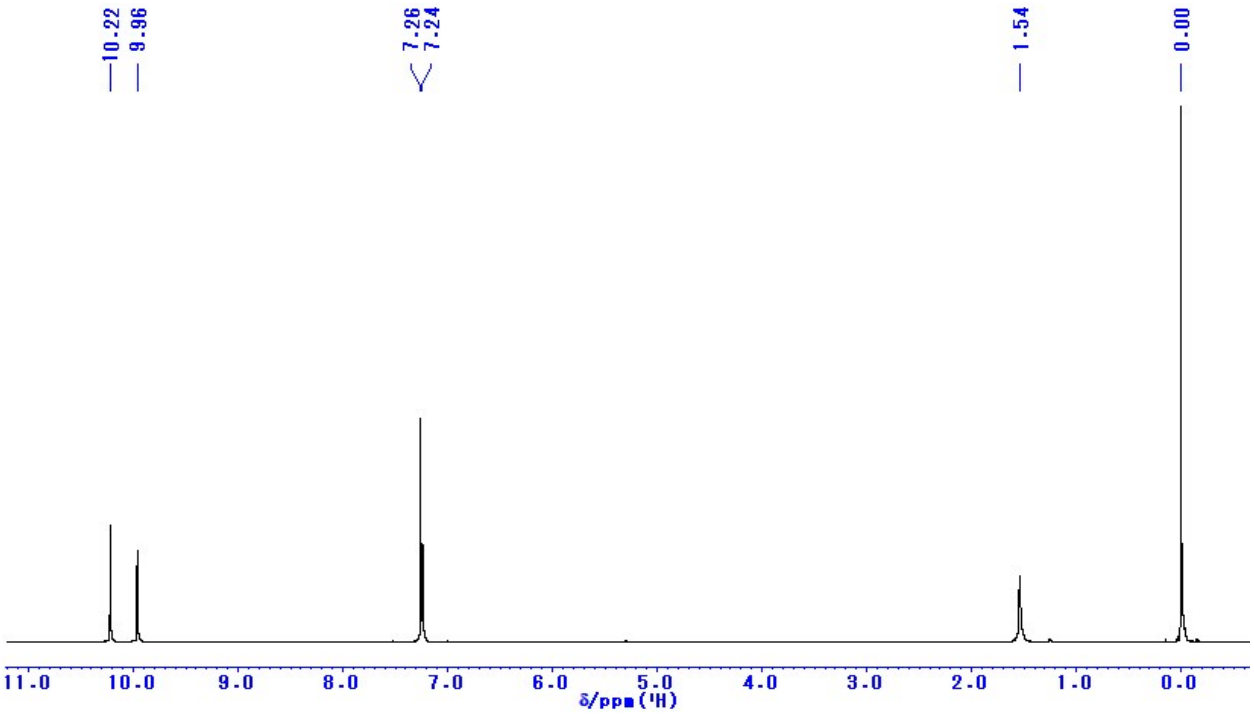

Fig. S3. ^{1}H NMR spectrum of **2**, $CDCl_3$, 400 MHz.

Synthesis of 3, *syn*- and *anti*-bisBAm

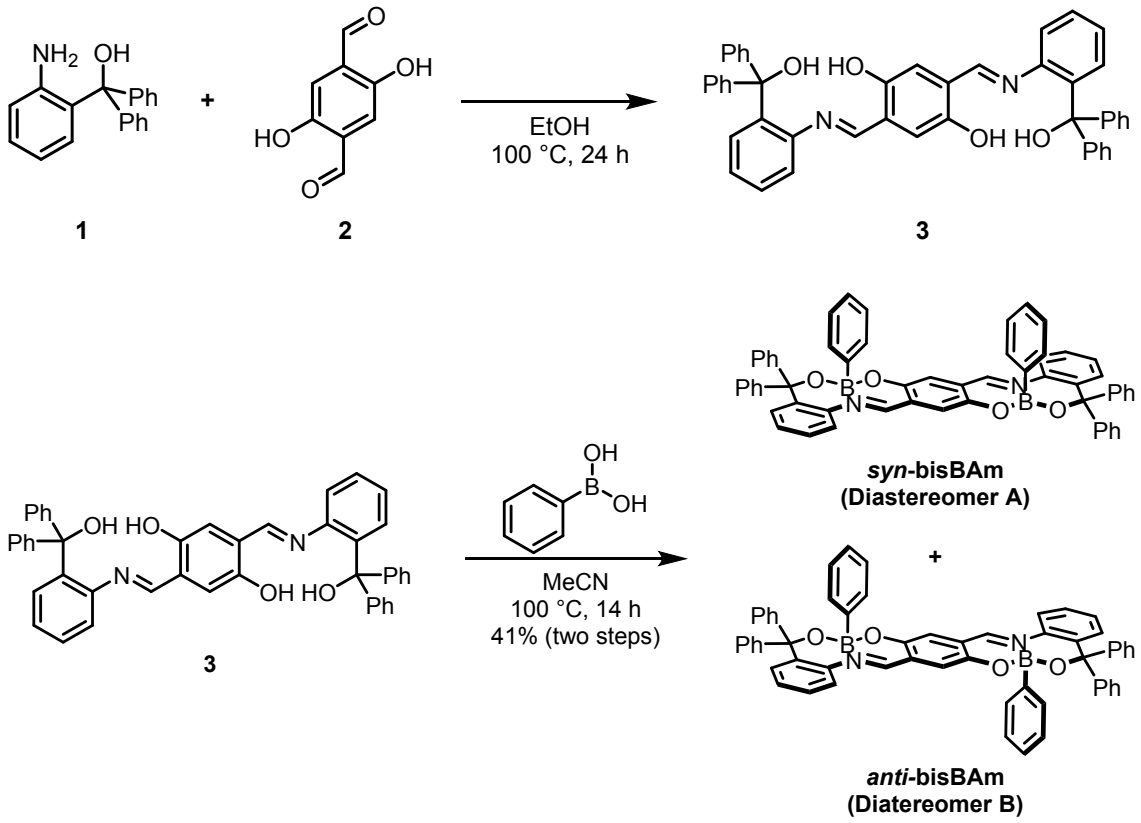

Scheme S3. Synthesis of ***syn*-** and ***anti*-bisBAm**.

1 (0.27 g, 0.96 mmol) and **2** (0.08 g, 0.48 mmol) were dissolved in EtOH (10 mL) and refluxed for 24 h. During course of the reaction, the product was precipitated from the reaction mixture. After cooling to room temperature, the precipitation was collected by filtration and dried in vacuo to give **3** as a white solid. The crude product was used in the next step without any further purification (0.31 g, 0.45 mmol).

3 (0.37 g, 0.54 mmol) was dissolved in MeCN (5.4 mL) at reflux temperature. Phenylboronic acid (0.13 g, 1.07 mmol) was added to the reaction mixture and refluxed for 14 h. After cooling to room temperature, the solvent was removed by a rotary evaporator to give a deep blue solid. ^{1}H NMR analysis of the crude material which was purified by column chromatography on SiO_2 (CH_2Cl_2 as an eluent) revealed that ***syn*-bisBAmPh** and ***anti*-bisBAm** were obtained. After reprecipitation with $CHCl_3$ and hexane (good and poor solvent, respectively), **bisBAm** was obtained as a mixture of diastereomers (0.20 g, 0.23 mmol, 14%, 2 steps from **1**). Further purification was carried out by following operations to separate ***syn*-bisBAm** and ***anti*-bisBAm**. Et_2O was added to the $CHCl_3$ solution of the diastereomers mixture and stirred for 1 h. After

the precipitation was collected by filtration, the solvent was removed from filtrate to give ***syn*-bisBAm** as a deep blue powder. The precipitation was purified by reprecipitation with $CHCl_3$ and Et_2O (good and poor solvent, respectively) again to afford ***anti*-bisBAm** as a deep blue powder.

R_f = 0.47 (CH_2Cl_2). HRMS (ESI): Calcd for $[M+Na]^+$, 875.3223; found, m/z 875.3231.

***syn*-bisBAm:** ^{1}H NMR ($CDCl_3$, 400 MHz), δ (ppm): 8.05 (s, 2H), 7.51–6.85 (m, 40H). ^{11}B NMR ($CDCl_3$, 128 MHz), δ (ppm): 4.91. ^{13}C NMR ($CDCl_3$, 100 MHz), δ (ppm): 157.9, 152.2, 146.7, 146.5, 143.0, 139.8, 131.7, 129.4, 129.4, 129.2, 128.8, 128.8, 128.0, 127.6, 127.5, 127.5, 127.4, 127.2, 124.5, 120.6, 120.4, 82.4.

***anti*-bisBAm:** ^{1}H NMR ($CDCl_3$, 400 MHz), δ (ppm): 8.04 (s, 2H), 7.48–6.83 (m, 40H). ^{11}B NMR ($CDCl_3$, 128 MHz), δ (ppm): 4.81. ^{13}C NMR ($CDCl_3$, 100 MHz), δ (ppm): 158.3, 152.1, 146.6, 146.4, 143.2, 139.8, 131.6, 129.4, 129.4, 129.2, 128.8, 128.7, 128.0, 127.6, 127.5, 127.5, 127.4, 127.2, 124.4, 120.5, 120.4, 82.4.

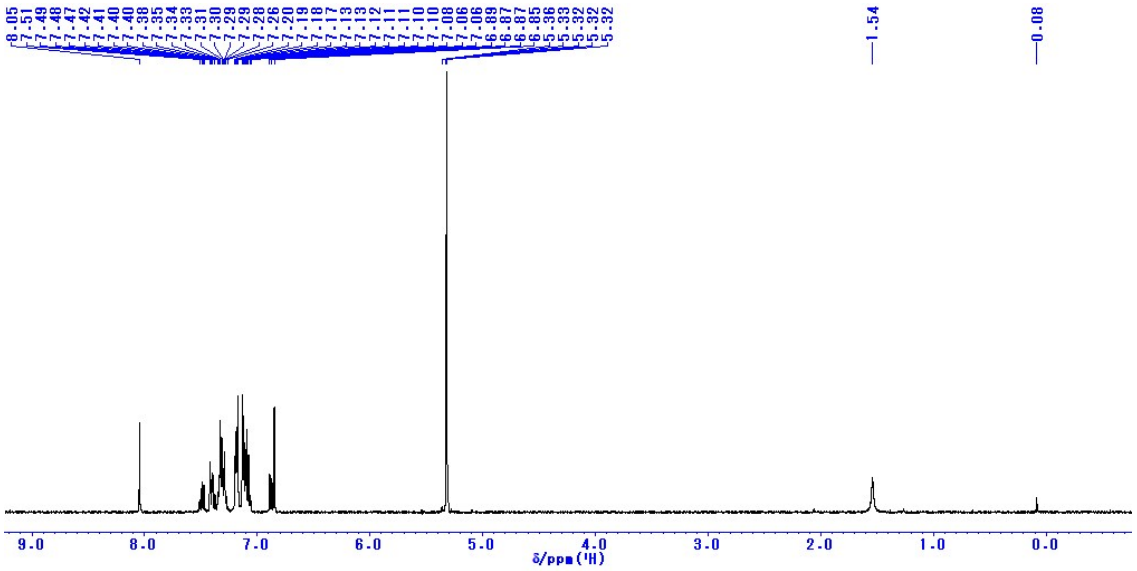

Fig. S4. ^{1}H NMR spectrum of ***syn*-bisBAm**, CD_2Cl_2, 400 MHz.

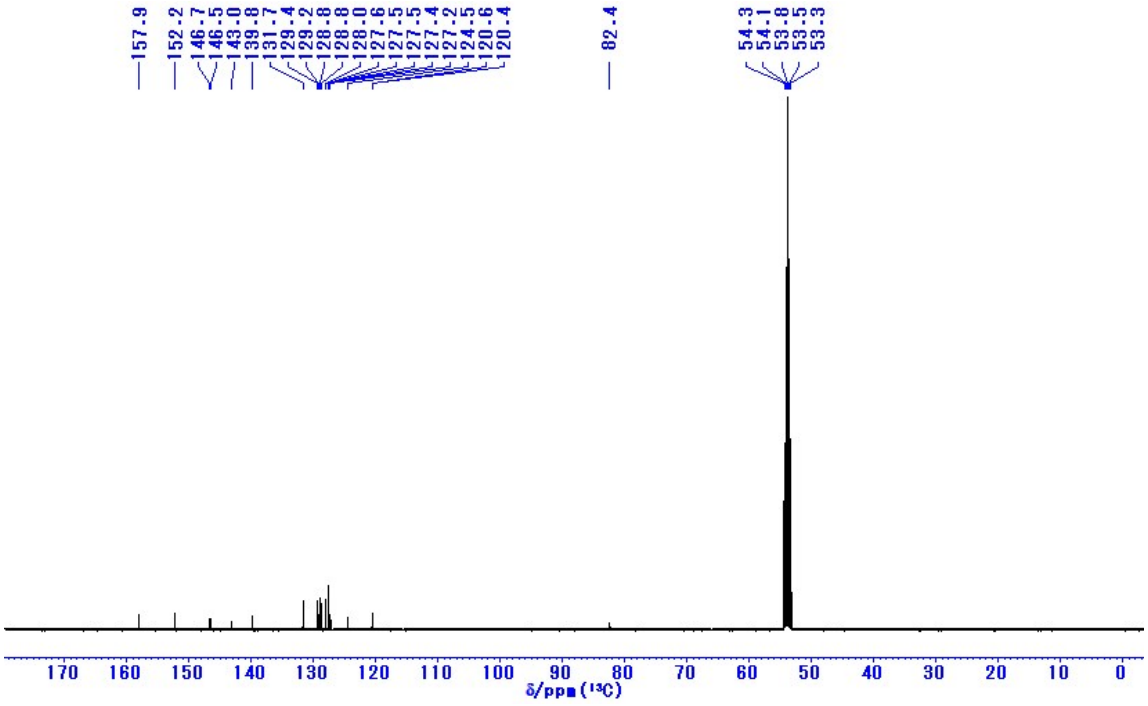

Fig. S5. ^{13}C NMR spectrum of ***syn*-bisBAm**, CD_2Cl_2, 100 MHz.

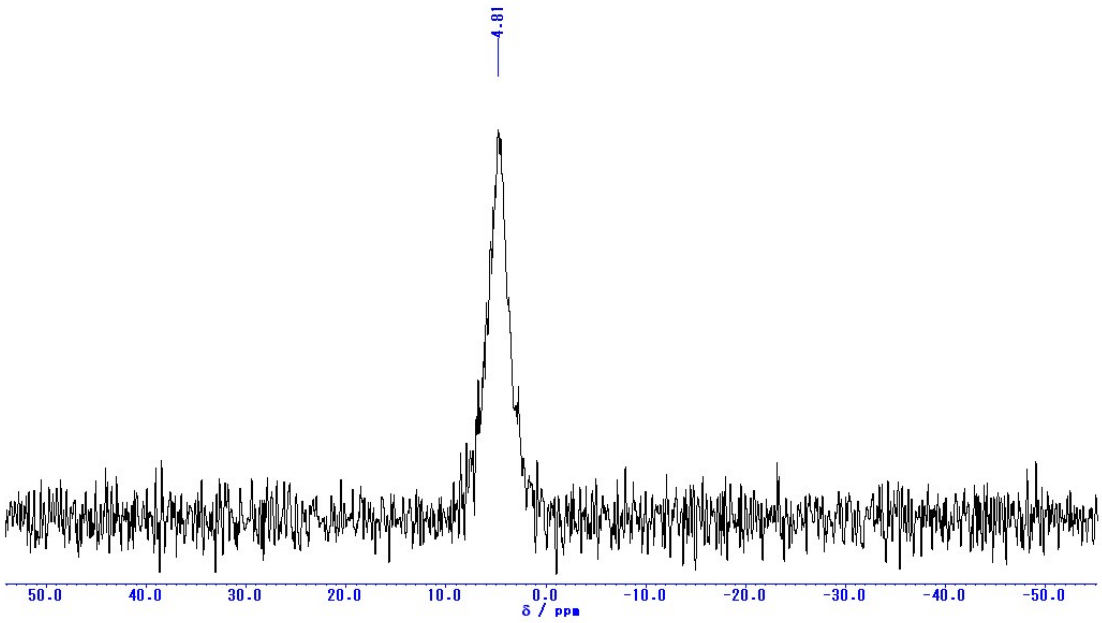

Fig. S6. ^{11}B NMR spectrum of ***syn*-bisBAm**, CD_2Cl_2, 128 MHz.

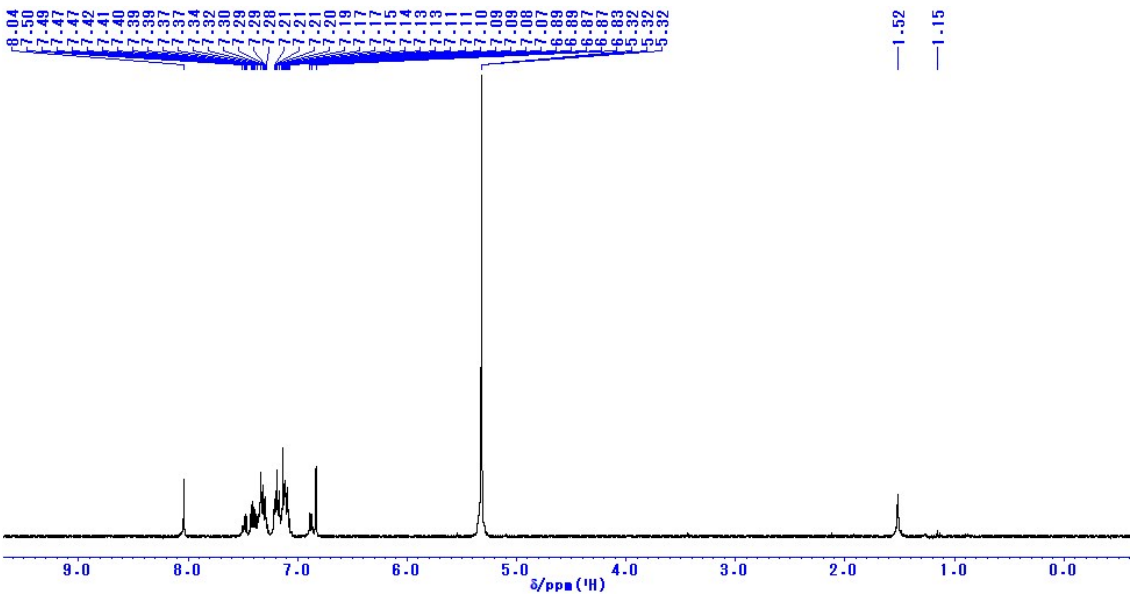

Fig. S7. ^{1}H NMR spectrum of ***anti*-bisBAm**, CD_2Cl_2, 400 MHz.

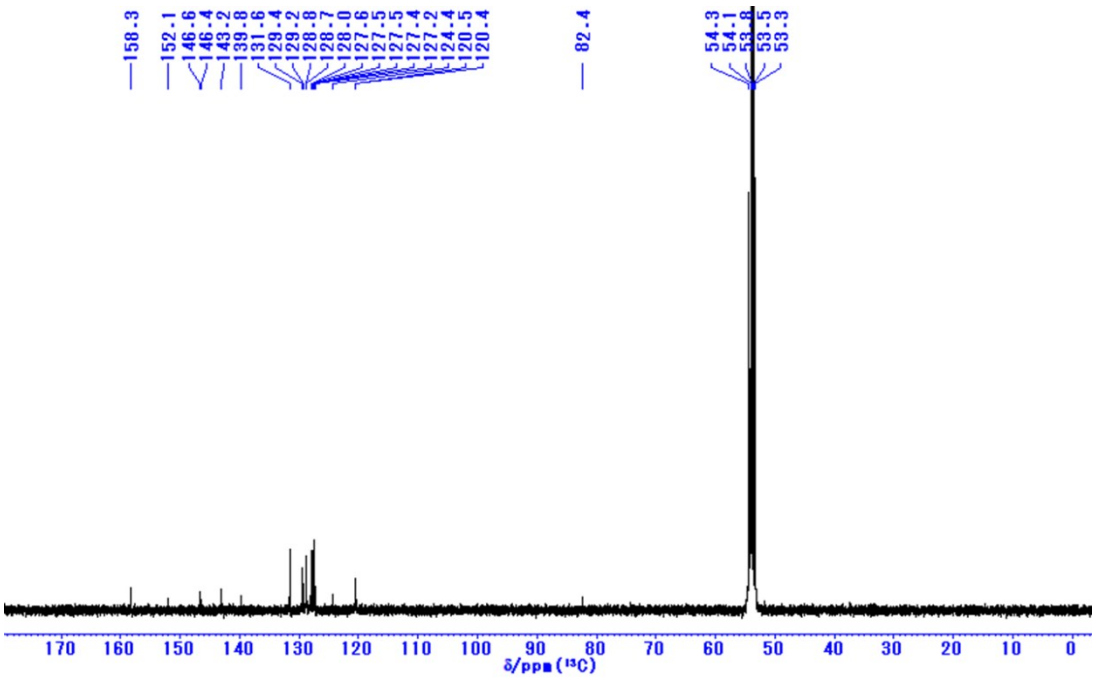

Fig. S8. ^{13}C NMR spectrum of ***anti*-bisBAm**, CD_2Cl_2, 100 MHz.

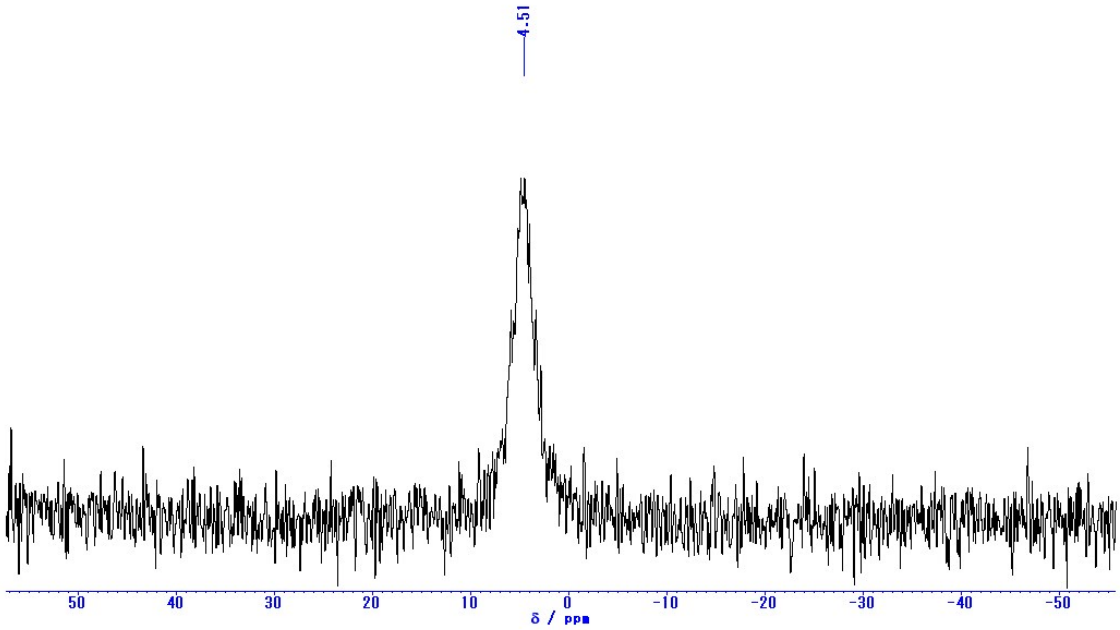

Fig. S9. ^{11}B NMR spectrum of ***anti*-bisBAm**, CD_2Cl_2, 128 MHz.

Synthesis of 4

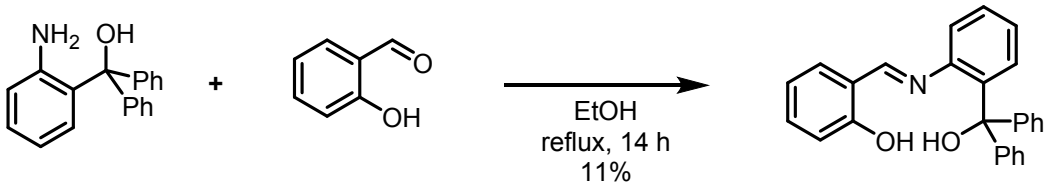

1 **Salicylaldehyde** **4**

Scheme S4. Synthesis of compound **4**.

1 (1.20 g, 4.37 mmol) and salicylaldehyde (0.53 g, 4.37 mmol) were dissolved in EtOH (27 mL) and refluxed for 14 h. During course of the reaction, the product was precipitated from the reaction mixture. The precipitation collected by filtration was purified by column chromatography on SiO_2 (hexane/EtOAc = 4/1 v/v as an eluent). The obtained white powder redissolved in a small amount of $CHCl_3$, and then the product was reprecipitated from hexane. The resulting precipitation collected by filtration was dried in vacuo to afford **4** (0.18 g, 0.47 mmol, 11%) as a white solid.

R_f = 0.45 (hexane/EtOAc = 4/1 v/v). ^{1}H NMR (DMSO-d_6, 400 MHz), δ (ppm): 9.49 (bs, 1H), 7.66 (d, 1H), 7.41−6.41 (m, 18H), 5.73 (s, 1H). ^{13}C NMR (DMSO-d_6, 100 MHz), δ (ppm): 154.8, 147.3, 145.1, 143.0, 129.3, 129.1, 128.8, 128.0, 127.8, 127.8, 127.6, 127.6, 127.4, 127.0, 125.7, 123.2, 118.9, 116.1, 115.4, 115.2, 84.3, 74.0. HRMS (ESI): Calcd for $[M+Na]^+$, 488.1792; found, m/z 488.1792.

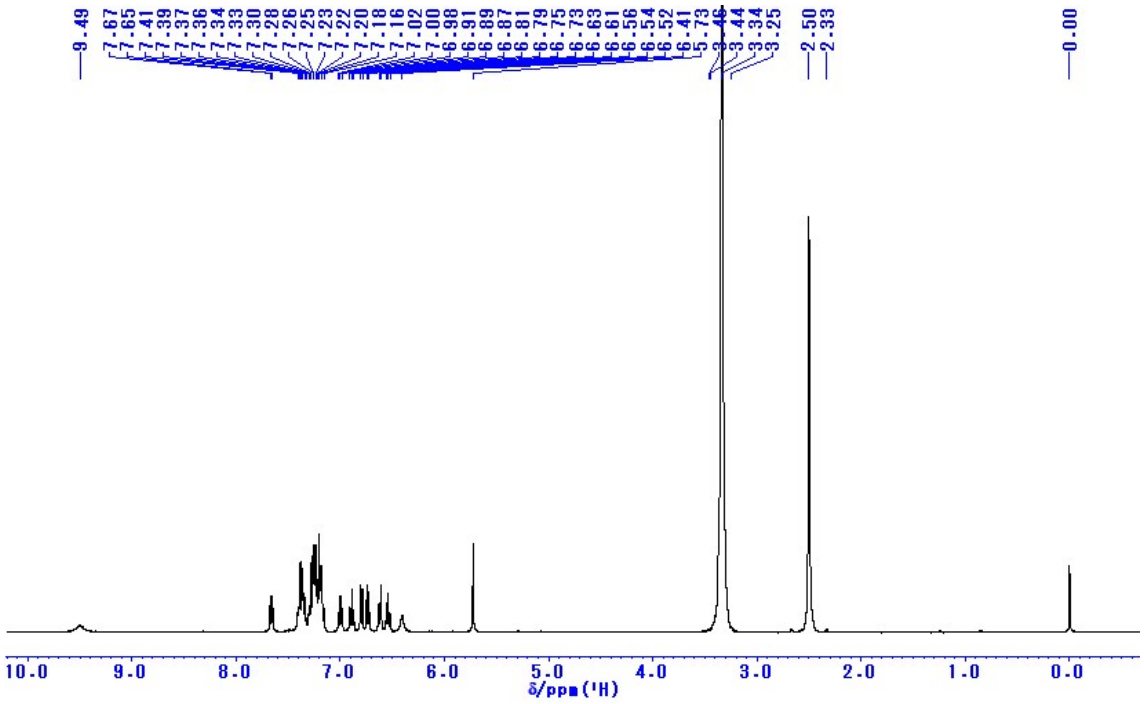

Fig. S10. ^{1}H NMR spectrum of **4**, DMSO-d_6, 400 MHz.

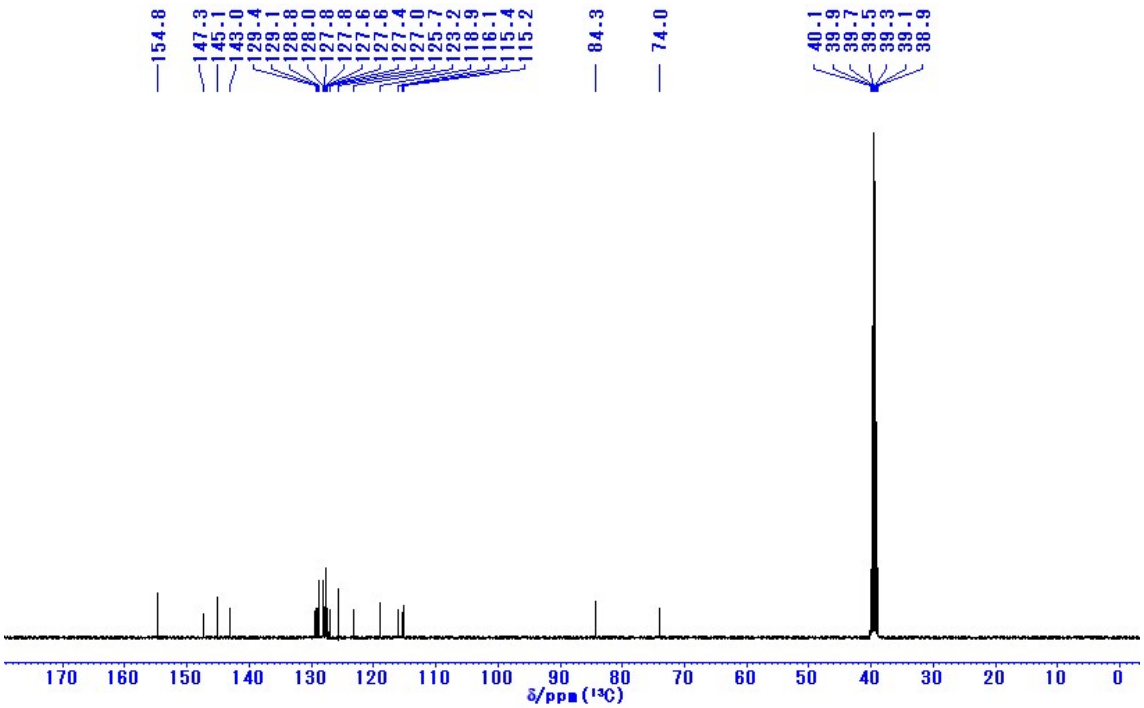

Fig. S11. ^{13}C NMR spectrum of **4**, DMSO-d_6, 100 MHz.

Synthesis of monoBAm

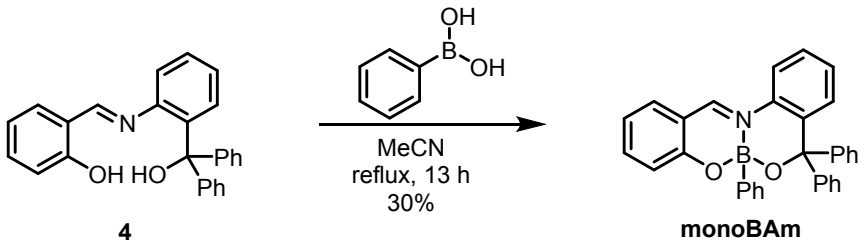

4 **monoBAm**

Scheme S5. Synthesis of **monoBAm**.

4 (0.10 g, 0.26 mmol) was dissolved in MeCN (2.6 mL) at reflux temperature. Phenylboronic acid (0.032 g, 0.26 mmol) was added to the reaction mixture and refluxed for 13 h. After cooling to room temperature, the solvent was removed by a rotary evaporator to give a yellow powder. The residue was purified by column chromatography on SiO_2 (hexane/EtOAc = 3/1 v/v as an eluent) and further purification was carried out by recrystallization with $CHCl_3$ and hexane (good and poor solvent, respectively) to afford **monoBAm** (0.037 g, 0.080 mmol, 30%) as an yellow crystal.

R_f = 0.43 (hexane/EtOAc = 3/1 v/v). ^{1}H NMR (CD_2Cl_2, 400 MHz), δ (ppm): 8.02 (s, 1H), 7.49–6.76 (m, 23H). ^{11}B NMR ($CDCl_3$, 128 MHz), δ (ppm): 4.61. ^{13}C NMR (CD_2Cl_2, 100 MHz), δ (ppm): 161.6, 158.5, 146.9, 146.6, 142.9, 140.1, 139.3, 132.4, 131.5, 131.5, 129.2, 129.1, 128.9, 128.8, 128.4, 128.0, 127.5, 127.4, 127.3, 127.0, 120.3, 119.7, 119.0, 116.8, 82.3. HRMS (ESI): Calcd for $[M+Na]^+$, 488.1792; found, m/z 488.1792.

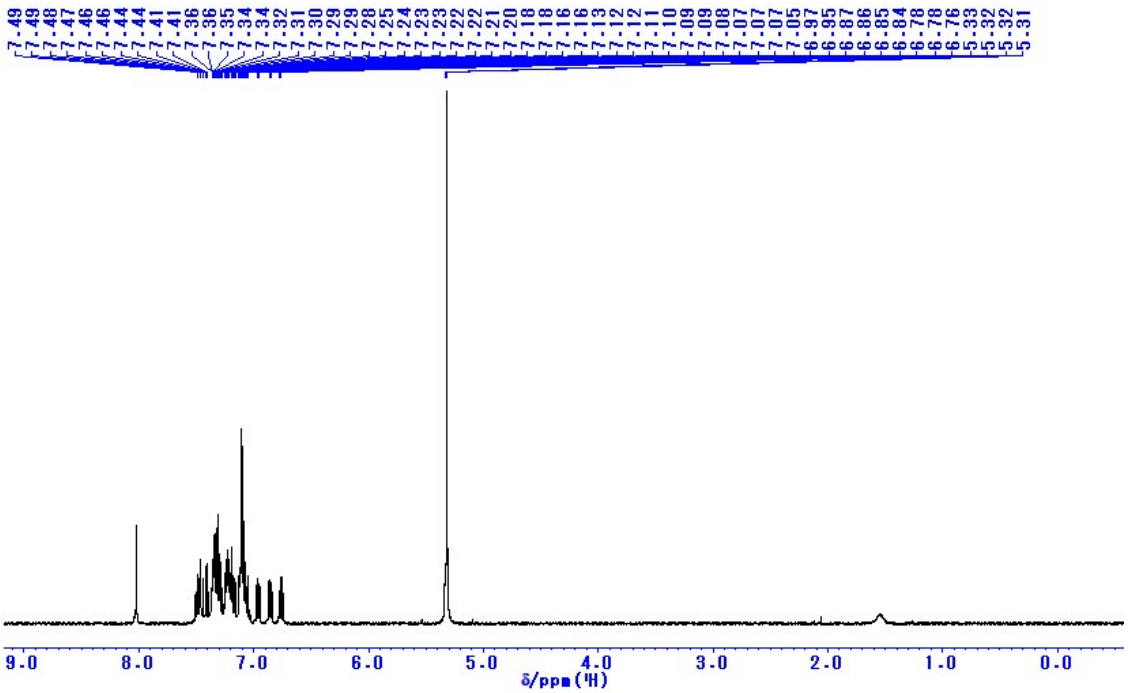

Fig. S12. ^{1}H NMR spectrum of **monoBAm**, CD_2Cl_2, 400 MHz.

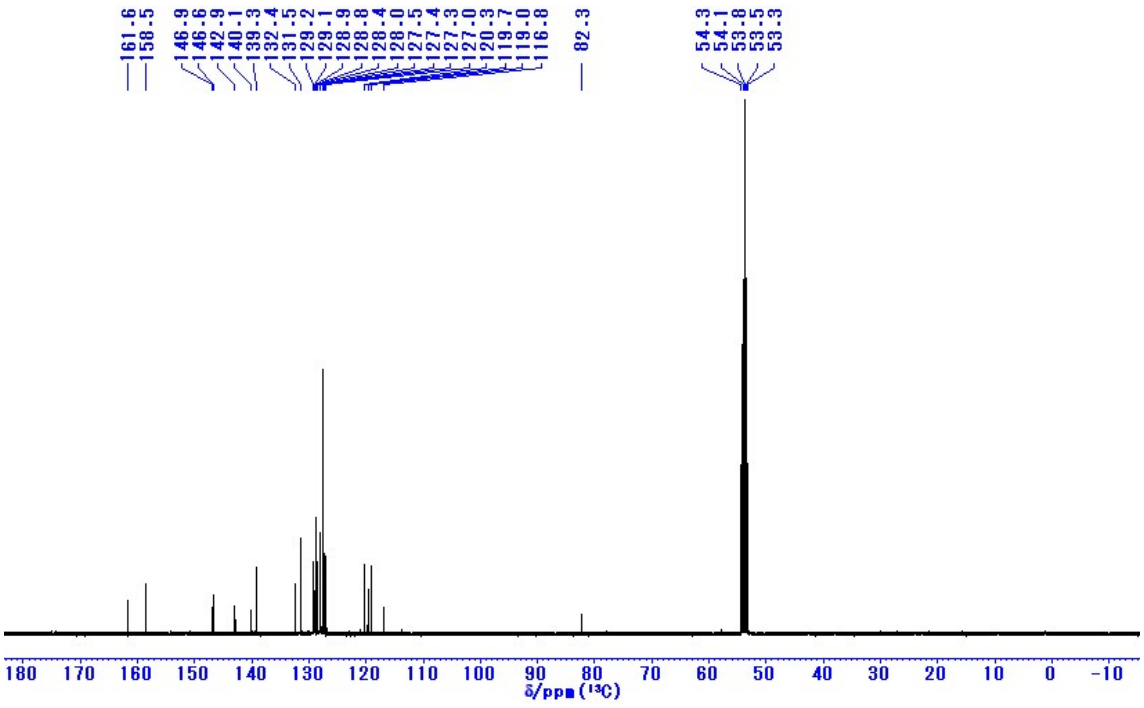

Fig. S13. ^{13}C NMR spectrum of **monoBAm**, CD_2Cl_2, 100 MHz.

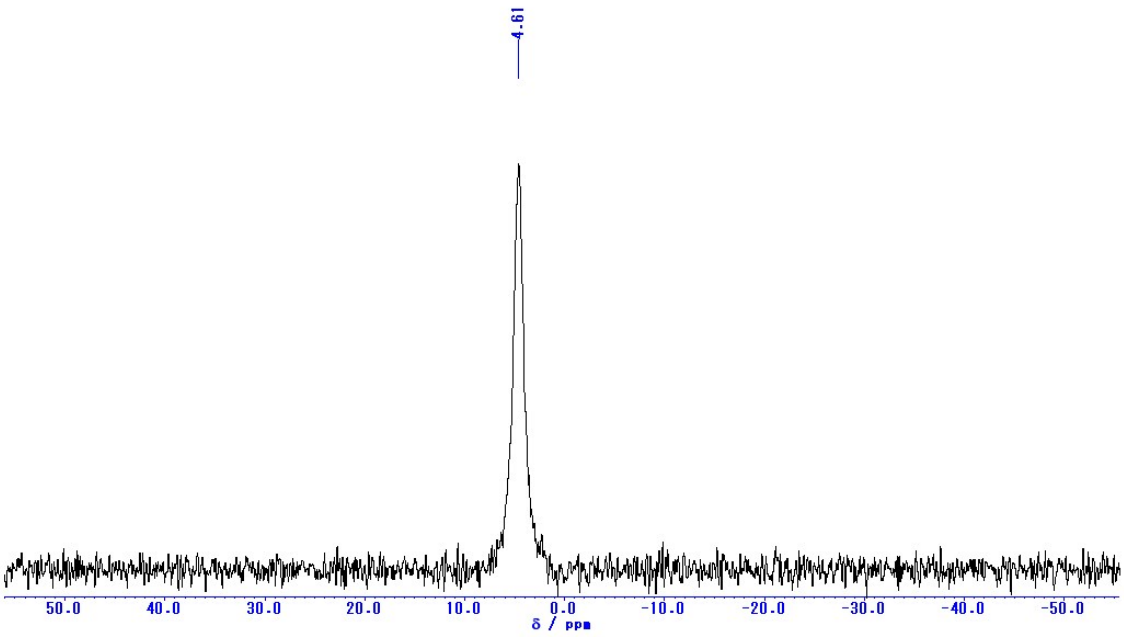

Fig. S14. ^{11}B NMR spectrum of **monoBAm**, CD_2Cl_2, 128 MHz.

Synthesis of 5

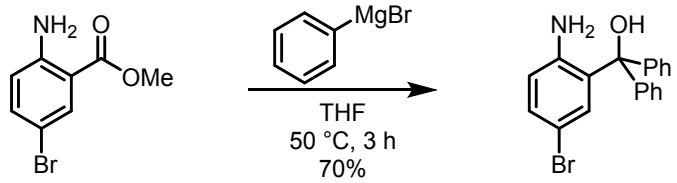

Methyl 5-bromoanthranilate **5**

Scheme S6. Synthesis of compound **5**.

Phenylmagnesium bromide (1.0 M in THF) was prepared prior to use. Mg (3.34 g, 139 mmol) in dry THF was activated with I_2 under argon atmosphere. Phenyl bromide (11 mL, 104 mmol) in dry THF (104 mL) was added slowly into the solution. After addition was complete, the mixture was stirred at room temperature for 2 h. To a solution of methyl 5-bromo anthranilate (8.00 g, 34.8 mmol) in THF (33 mL) was added slowly into 1.0 M phenylmagnesium bromide in THF (104 mL) at 0 °C. The mixture was heated to 50 °C and stirred for 3 h. After cooling to room temperature, the mixture was quenched by 1.0 M HCl aqueous solution. Then, the product was extracted with EtOAc. Organic layers were washed with brine, dried over $MgSO_4$ and evaporated to afford a brown solid. The solid was purified by column chromatography on SiO_2 (hexane/EtOAc = 3/1 v/v as an eluent) and further purification was carried out by recrystallization with $CHCl_3$ and hexane (good and poor solvent, respectively) to afford **5** (8.64 g, 24.4 mmol, 70%) as a white powder.

R_f = 0.37 (hexane/EtOAc = 3/1 v/v). ^{1}H NMR (CD_2Cl_2, 400 MHz), δ (ppm): 7.38–7.21 (m, 11H), 6.62 (d, J = 8.4 Hz, 1H), 6.56 (d, J = 2.2 Hz, 1H). ^{13}C NMR (CD_2Cl_2, 100 MHz), δ (ppm): 145.4, 144.4, 134.7, 132.7, 13.18, 128.6, 128.0, 128.0, 120.4, 110.8, 82.5. HRMS (ESI): Calcd for $[M+Na]^+$, 376.0307; found, m/z 376.0308.

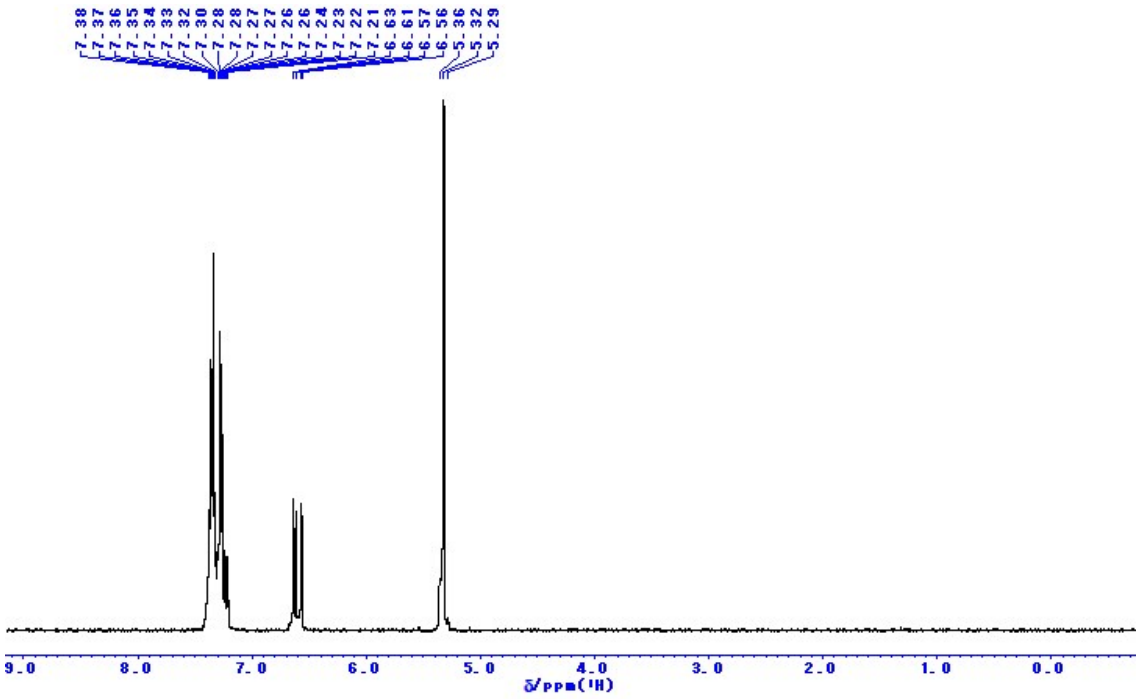

Fig. S15. ^{1}H NMR spectrum of **5**, CD_2Cl_2, 400 MHz.

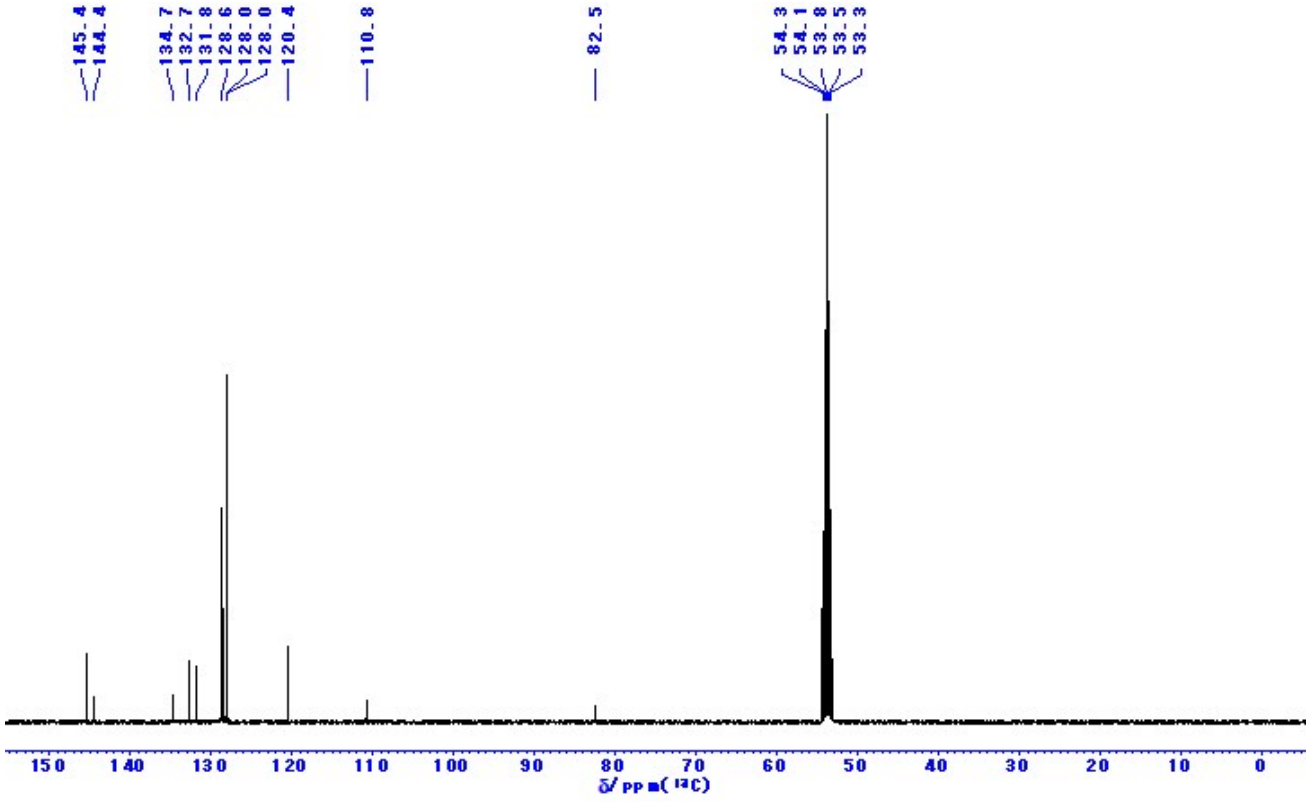

Fig. S16. ^{13}C NMR spectrum of **5**, CD_2Cl_2, 400 MHz.

Synthesis of 6 and bisBAmBr

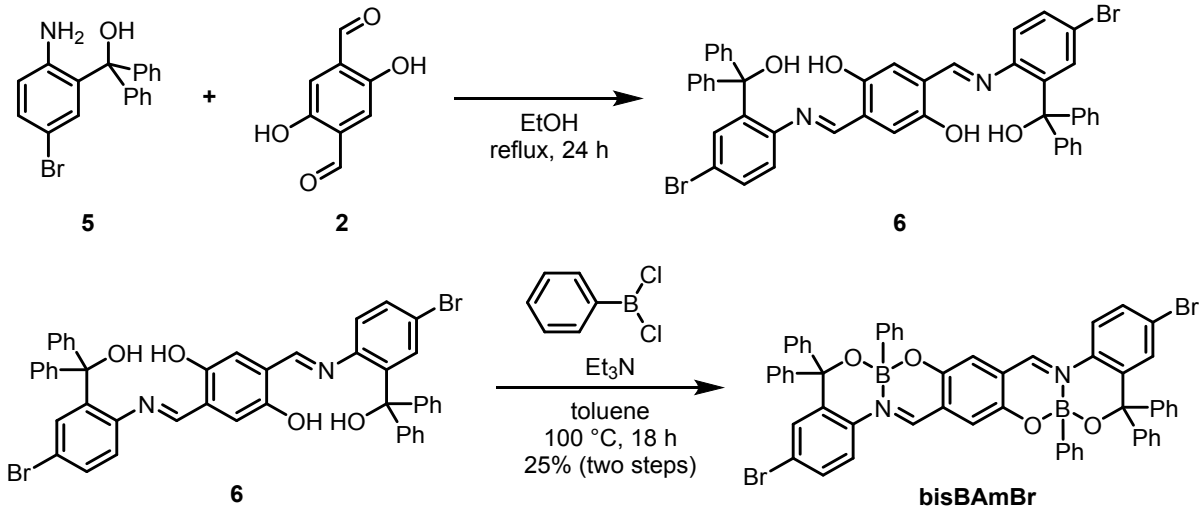

Scheme S7. Synthesis of **bisBAmBr**.

5 (3.13 g, 8.85 mmol) and **2** (0.73 g, 4.42 mmol) were dissolved in EtOH (37 mL) and refluxed for 24 h. During course of the reaction, the product was precipitated from the reaction mixture. After cooling to room temperature, the precipitation was collected by filtration and dried in vacuo to give **6** as a white solid. The crude product was used in the next step without any further purification (2.19 g, 2.61 mmol).

6 (0.42 g, 0.50 mmol) was dissolved in toluene (30 mL) under nitrogen atmosphere at 100 ℃ and triethylamine (0.2 mL, 1.5 mmol) was then added to the reaction mixture. Dichlorophenylborane (0.4 mL, 3.0 mmol) was added and stirred for 18 h. After cooling to room temperature, the precipitation was collected by filtration, washed with toluene and hexane, and then dried in vacuo to give a deep blue solid. The deep blue residue was purified by recrystallization with CH_2Cl_2 to afford **bisBAmBr** (0.22 g, 25%, 2 steps from **2**) as a deep blue powder.

R_f = 0.49 (CH_2Cl_2). ^{1}H NMR (CD_2Cl_2, 400 MHz), δ (ppm): 8.02 (s, 1H), 8.01 (s, 1H), 7.64–6.82 (m, 38H). ^{11}B NMR ($CDCl_3$, 128 MHz), δ (ppm): 5.01. ^{13}C NMR (CD_2Cl_2, 100 MHz), δ (ppm): 158.2, 152.3, 145.8, 145.8, 145.2, 138.8, 132.6, 132.2, 131.6, 128.7, 128.7, 128.2, 127.8, 127.7, 127.6, 127.6, 127.5, 124.5, 123.9, 122.2, 120.6, 82.3. HRMS (ESI): Calcd for $[M+Na]^+$, 1031.1433; found, m/z 1031.1453.

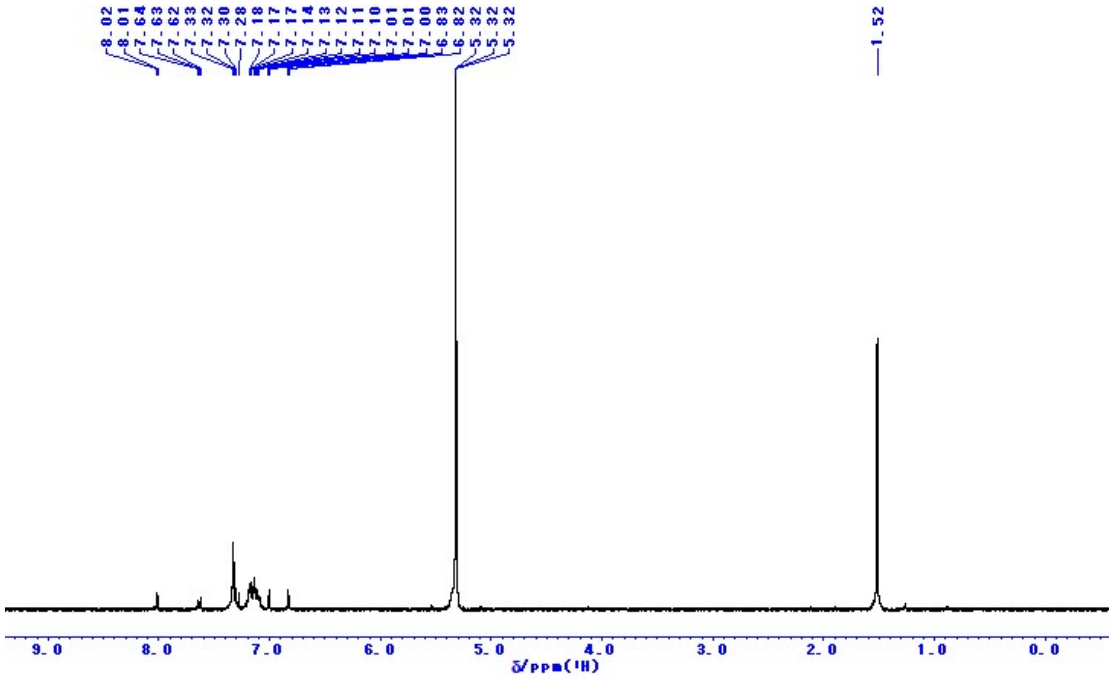

Fig. S17. ^{1}H NMR spectrum of **bisBAmBr**, CD_2Cl_2, 400 MHz.

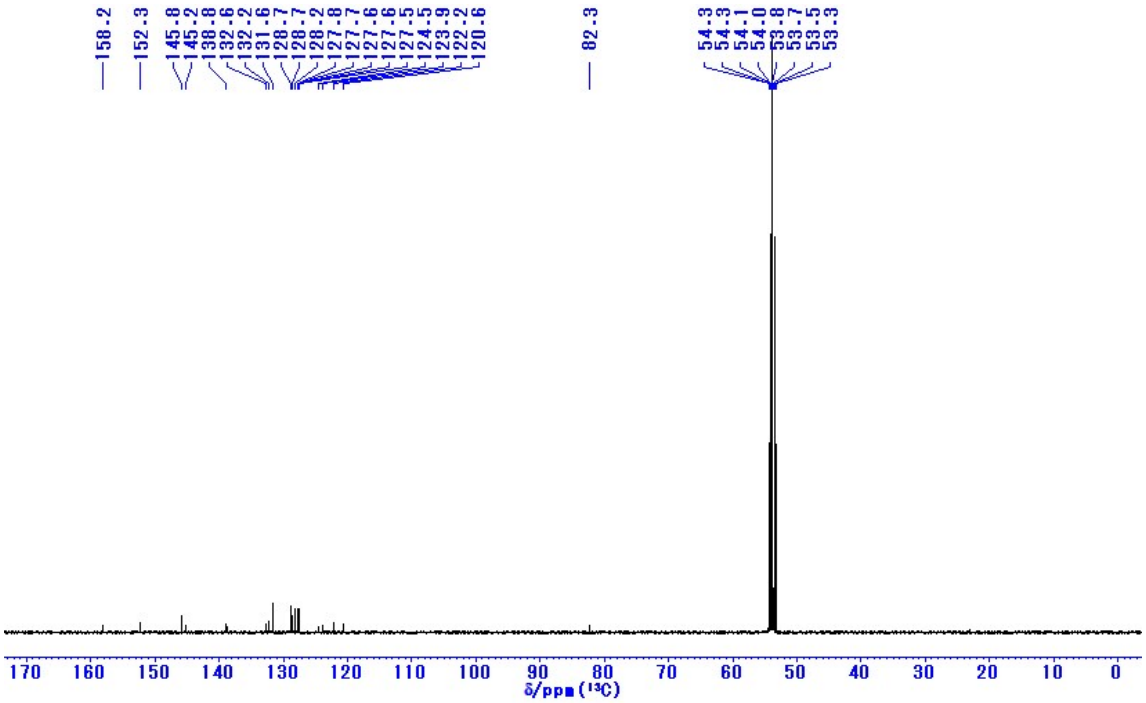

Fig. S18. ^{13}C NMR spectrum of **bisBAmBr**, CD_2Cl_2, 100 MHz.

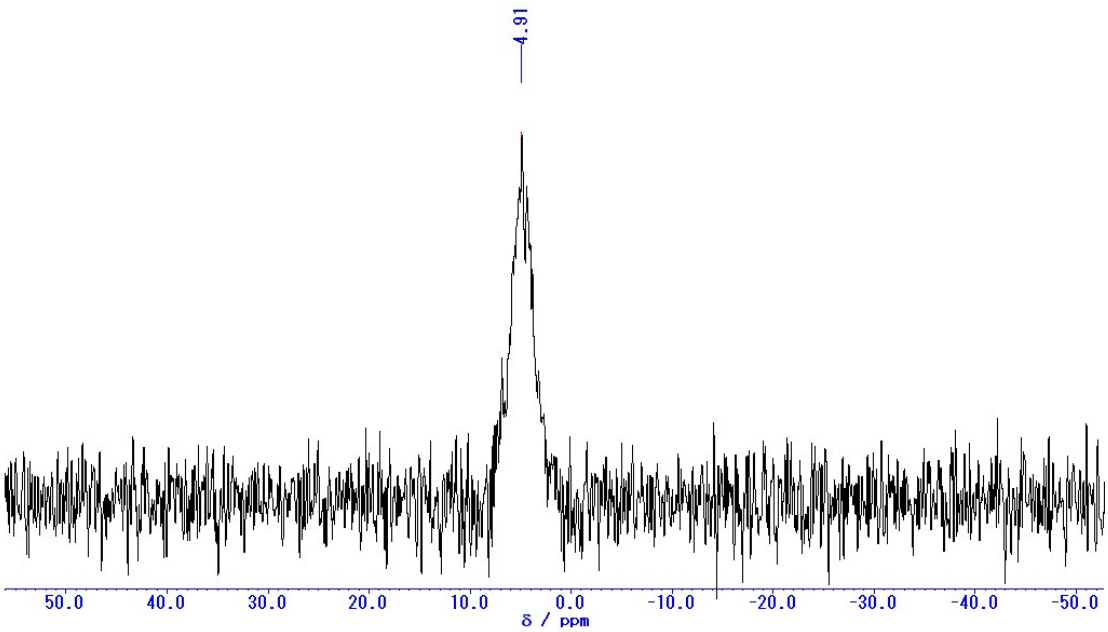

Fig. S19. ^{11}B NMR spectrum of **bisBAmBr**, CD_2Cl_2, 128 MHz.

Synthesis of p-bisBAm-F

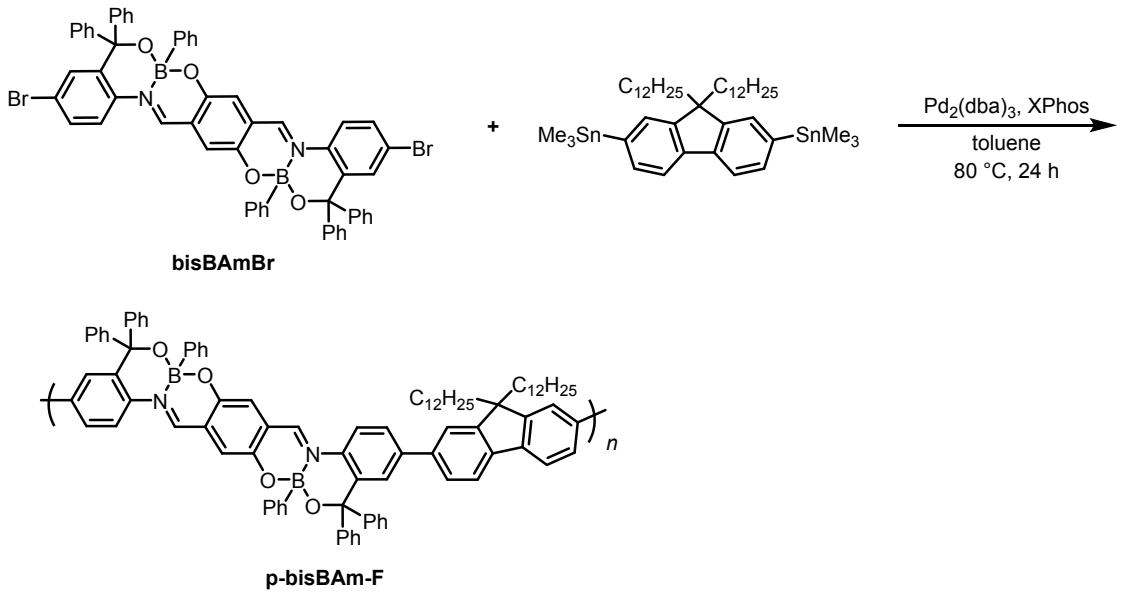

Scheme S8. Synthesis of **p-bisBAm-F**.

The mixture of **bisBAmBr** (101 mg, 0.10 mmol), (9,9-didodecyl-9*H*-fluorene-2,7-diyl)bis(trimethylstannane) (82.8 mg, 0.10 mmol), $Pd_2(dba)_3$ (2.7 mg, 0.0030 mmol), X-Phos (2.8 mg, 0.0060 mmol) in toluene (2.0 mL) was stirred at 80 °C for 24 h under N_2 atmosphere. After cooling to room temperature, the solvent was removed by rotary evaporator. The residue was dissolved into $CHCl_3$ and purified by alumina column chromatography. The solution was poured into a large amount of methanol to collect the polymer by filtration. The polymer collected by filtration was dried *in vacuo* to afford **p-bisBAm-F** as a red solid (115 mg, 85%).

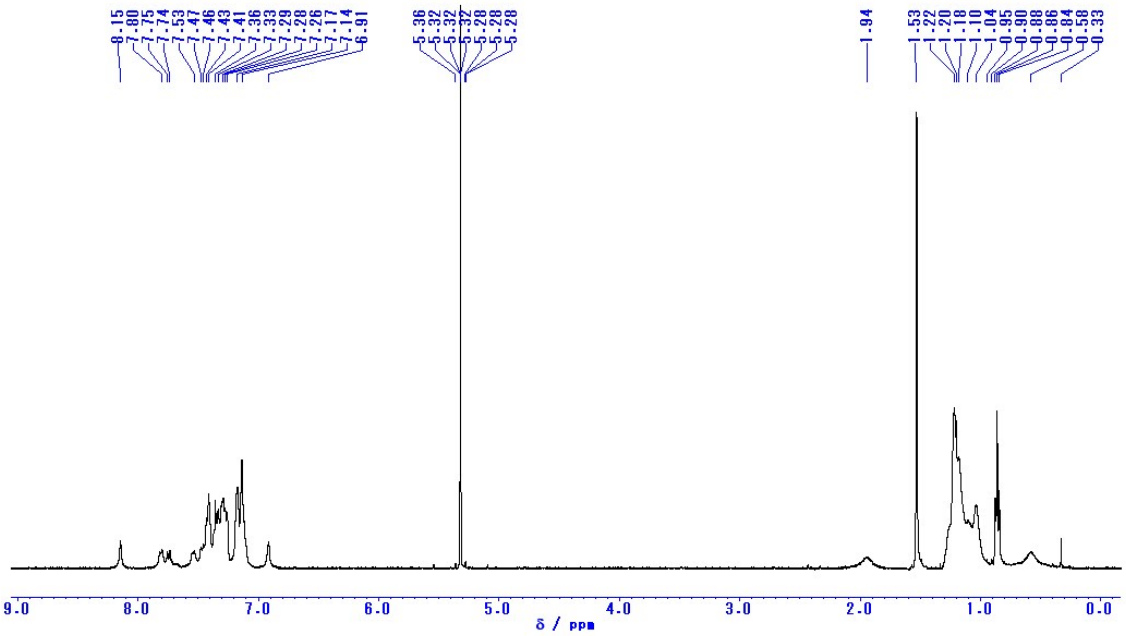

Fig. S20. ^{1}H NMR spectrum of **p-bisBAm-F**, CD_2Cl_2, 400 MHz.

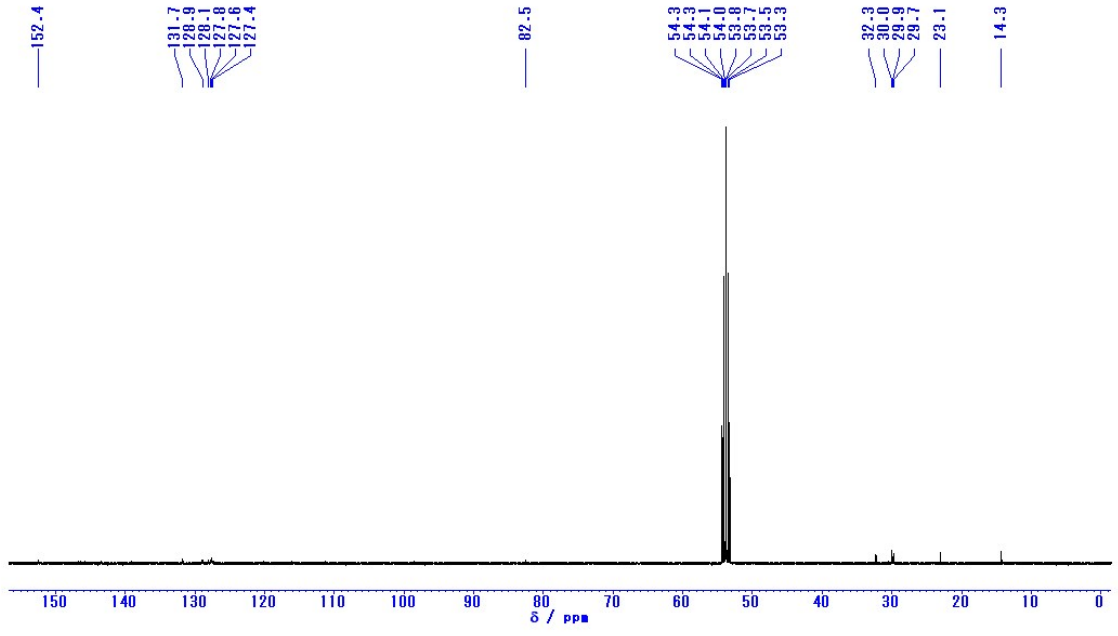

Fig. S21. ^{13}C NMR spectrum of **p-bisBAm-F**, CD_2Cl_2, 100 MHz.

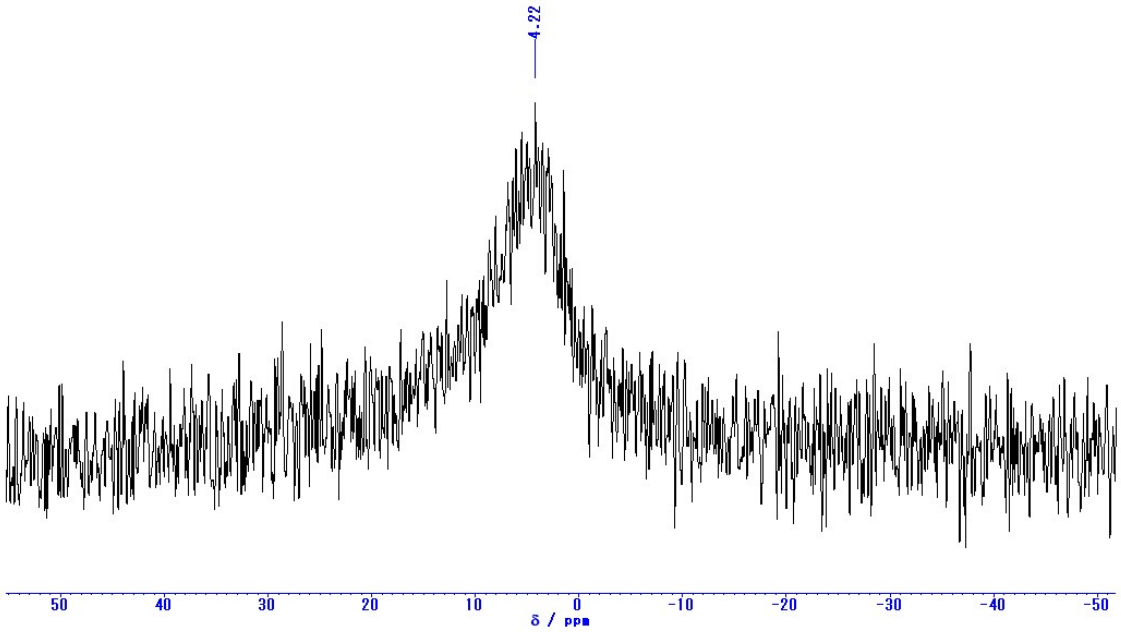

Fig. S22. ^{11}B NMR spectrum of **p-bisBAm-F**, CD_2Cl_2, 128 MHz.

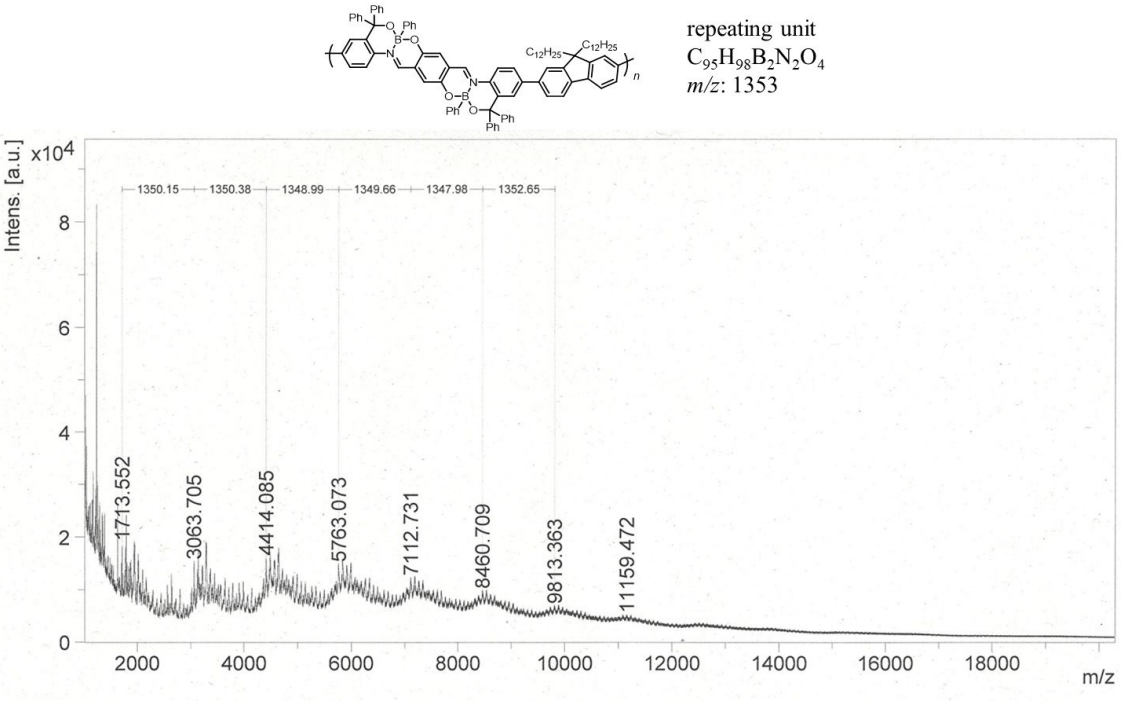

Fig. S23. MALDI-TOF mass spectrum of **p-bisBAm-F**.

Synthesis of p-bisBAm-T

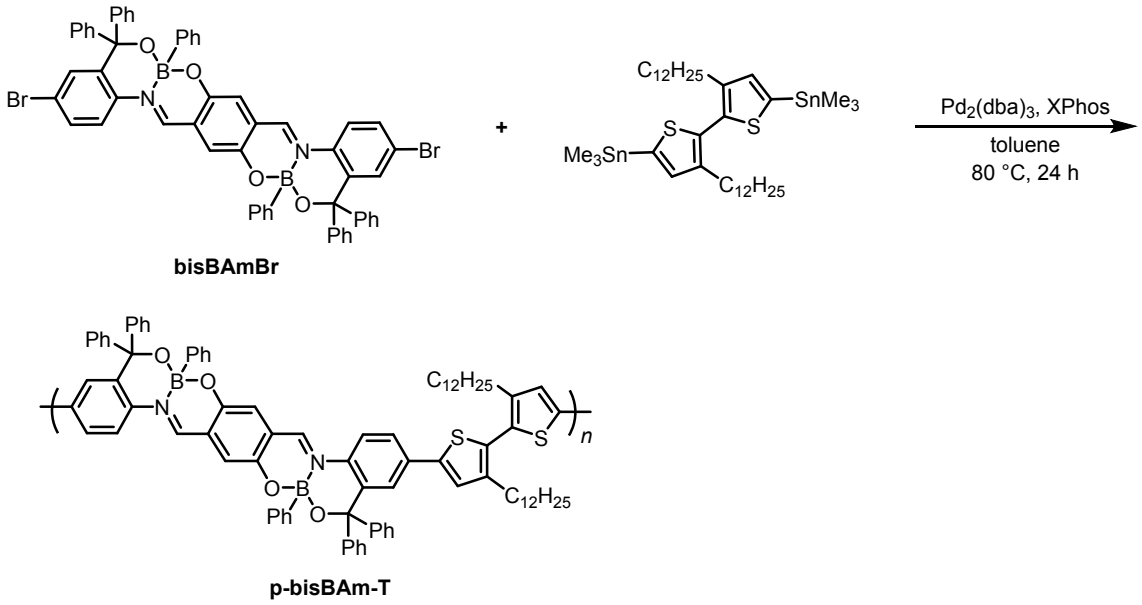

Scheme S9. Synthesis of **p-bisBAm-T**.

The mixture of **bisBAmBr** (101 mg, 0.10 mmol), (3,3′-didodecyl-[2,2′-bithiophene]-5,5′-diyl)bis(trimethylstannane) (82.9 mg, 0.10 mmol), $Pd_2(dba)_3$ (2.7 mg, 0.0030 mmol), X-Phos (2.8 mg, 0.0060 mmol) in toluene (2.0 mL) was stirred at 80 °C for 24 h under N_2 atmosphere. After cooling to room temperature, the solvent was removed by rotary evaporator. The residue was dissolved into $CHCl_3$ and purified by alumina column chromatography. The solution was poured into a large amount of methanol to collect the polymer by filtration. The polymer collected by filtration was dried *in vacuo* to afford **p-bisBAm-T** as a red solid (120 mg, 89%).

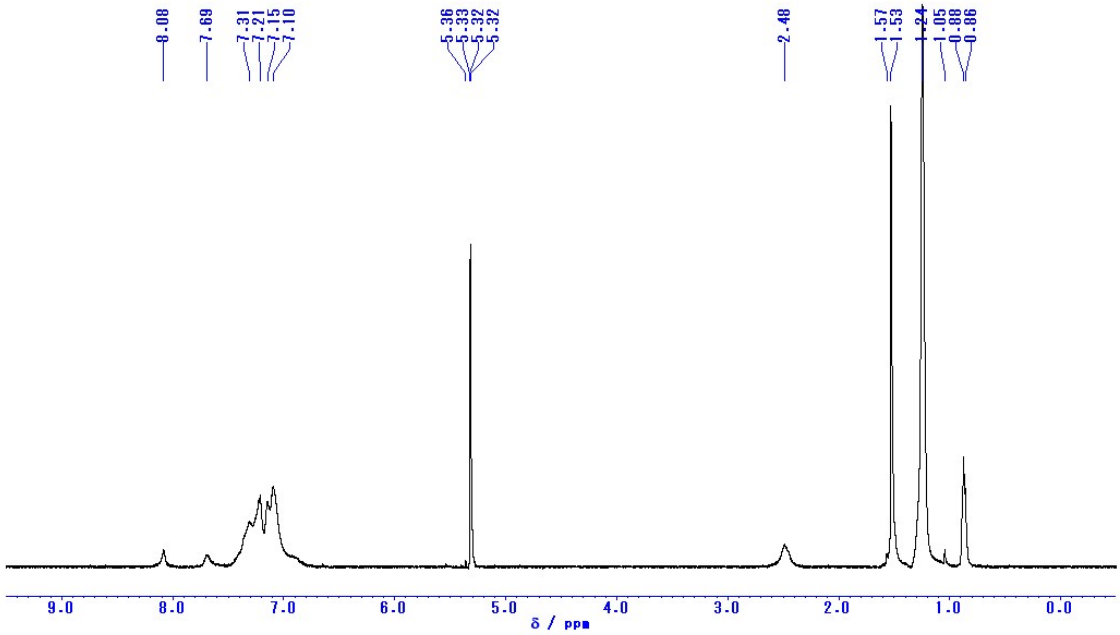

Fig. S24. ^{1}H NMR spectrum of **p-bisBAm-T**, CD_2Cl_2, 400 MHz.

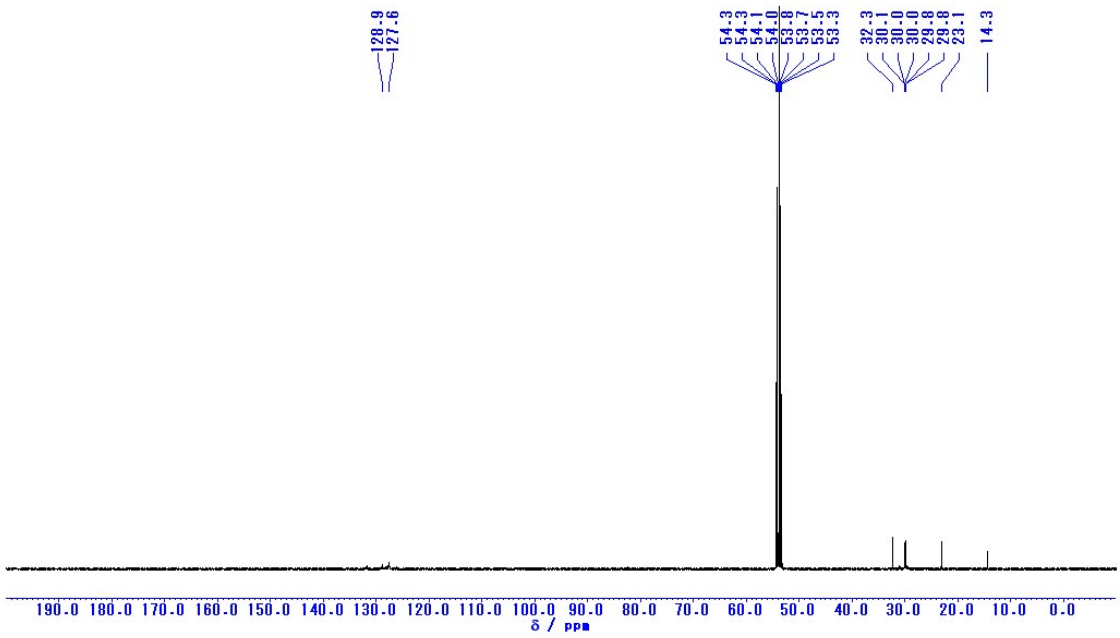

Fig. S25. ^{13}C NMR spectrum of **p-bisBAm-T**, CD_2Cl_2, 100 MHz.

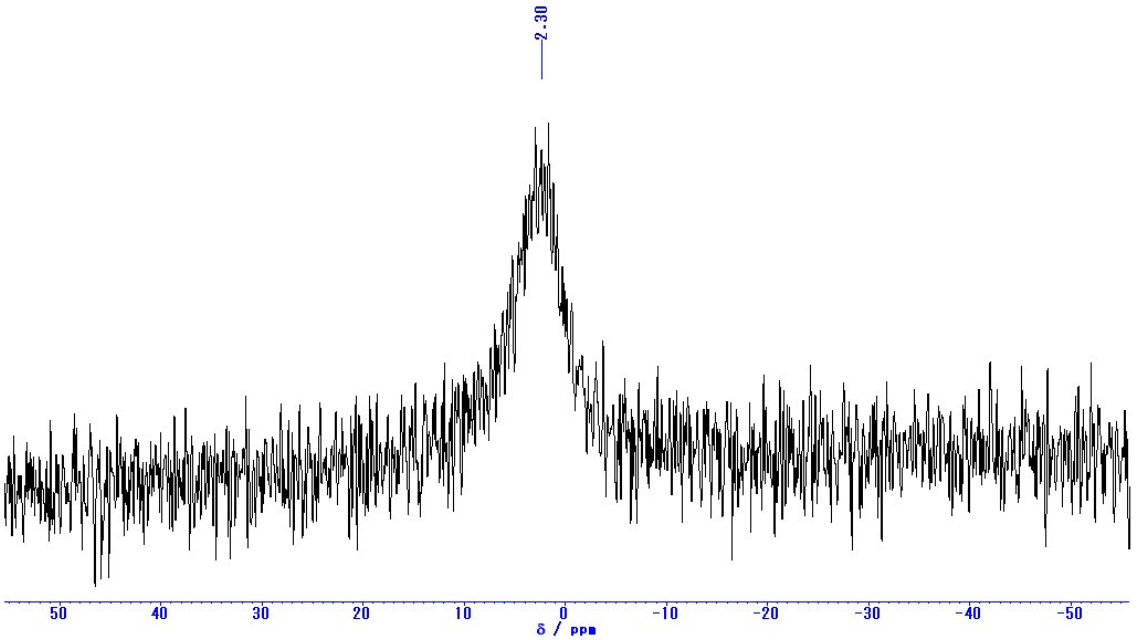

Fig. S26. ^{11}B NMR spectrum of **p-bisBAm-T**, CD_2Cl_2, 128 MHz.

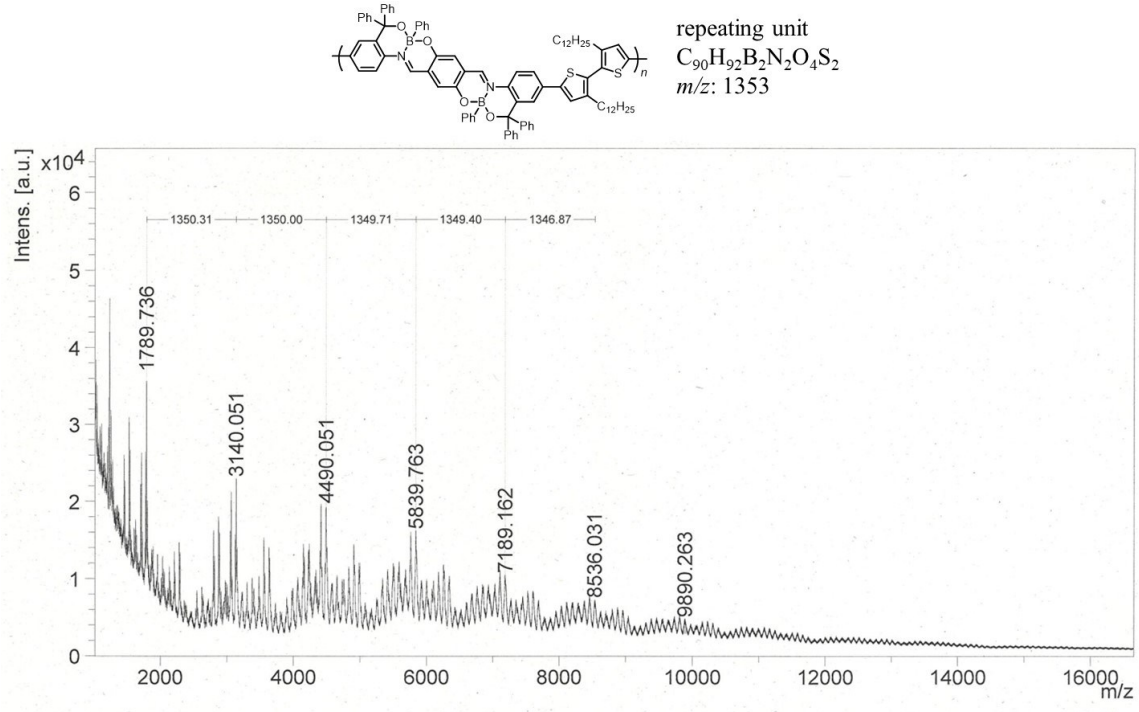

Fig. S27. MALDI-TOF mass spectrum of **p-bisBAm-T**.

^{1}H NMR spectra of bisBAm mixture, *syn*-bisBAm and *anti*-bisBAm

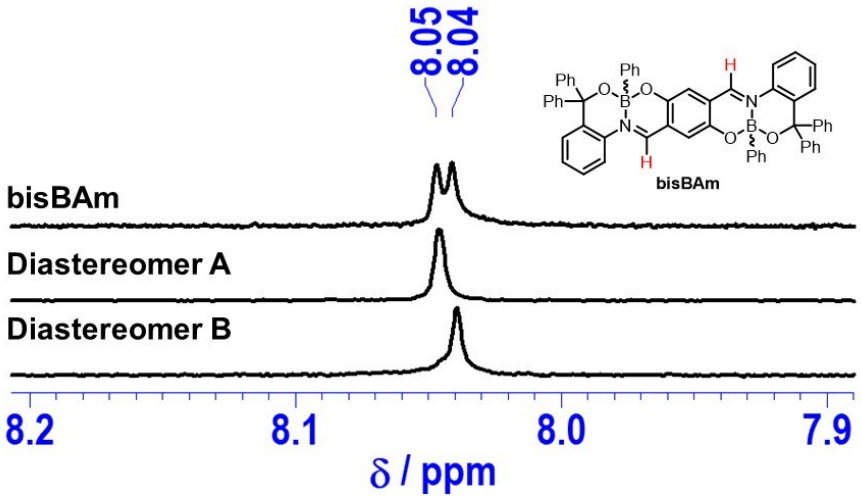

Fig. S28. Expanded ^{1}H NMR spectra (CD_2Cl_2, 400 MHz) of azomethine proton region in diastereomeric mixture **bisBAm**, separated Diastereomer A and Diastereomer B.

X-ray crystal structure analysis of *anti*-bisBAm

Intensity data were collected on a Rigaku R-AXIS RAPID imaging plate area detector with graphite monochromated MoKα radiation (λ = 0.71069 Å). The structures were solved and refined by full-matrix least-squares procedures based on F^2 (SHELXL-2014/7). Although R-factor was still high after refinement, there seemed to be no systematic error in the structure determination because the value was below 10%

Table S1. Crystallographic data of ***anti*-bisBAm** at 106 K

Morphology	blue needles
Space group	*P21/c*
a/Å	17.8827(11)
b/Å	7.8947(5)
c/Å	15.7916(10)
α/deg	90
β/deg	96.353(7)
γ/deg	90
V/Å^3	2215.7(2)
Z	2
Density/g cm^{-3}	1.278
Absorption coefficient	0.079
F(000)	892
Crystal size (nm)	0.300× 0.300× 0.200
θ range for data collection	2.596–27.386
Limiting indices	-23≤h≤23, -9≤k≤10, -20≤l≤20
Reflections collected (unique)	5005/3378 [R(int) = 0.1176]
Completeness to theta = 27.386	0.995
Max. and min. transmission	1.205 and 0.795
Goodness-off-fit on F^2	1.144
Final R indices [I > 2σ(I)][a]	R_1 = 0.0978 wR_2 = 0.1732
R indices (all data)	R_1 = 0.1561 wR_2 = 0.1953
T/K	106

[a] R1 = $\Sigma(|F_o|-|F_c|)/\Sigma|F_o|$. wR2 = $[\Sigma w(F^2_o-F^2_c)2/\Sigma w(F^2_o)^2]^{1/2}$. w = $1/[\sigma^2(F^2_o)+[(ap)^2+bp]]$, where p = $[\max(F^2_o,0)+2F^2_c]/3$.

Optical measurement data

Table S2. Detail optical properties of synthesized compounds[a]

	$\lambda_{max,abs}$ (nm)[b]	ε (10^4 M^{-1} cm^{-1})[c]	λ_{em} (nm)[d]	Stokes shift (cm^{-1})[e]	Φ_F[f]	τ (ns)[g]	χ^2	k_r ($\times 10^8$ s^{-1})[h]	k_{nr} ($\times 10^8$ s^{-1})[h]
monoBAm	419	0.65	522	4709	0.003	–	–	–	–
***syn*-bisBAm**	599	0.76	731	3015	0.035	1.5	1.06	0.23	6.2
***anti*-bisBAm**	595	0.95	729	3089	0.038	1.5	1.09	0.25	6.3
p-bisBAm-F	610	1.5	742	2916	0.060	1.4	1.16	0.47	6.6
p-bisBAm-T	614	2.0	742	2736	0.062	1.3	1.16	0.50	7.3

[a]$CHCl_3$ solution, 1.0×10^{-5} M (per repeating units in the case of polymer samples).
[b]The longest absorption maximum.
[c]Molar extinction coefficients at the longest absorption maximum.
[d]Fluorescence maxima with the excitation at the longest absorption maximum.
[e]The difference between the spectral positions of the band maxima of the absorption and emission.
[f]Absolute fluorescence quantum yield.
[g]Emission lifetime at λ_{em}.
[h]$k_r = \Phi_F/\tau$, $k_{nr} = (1 - \Phi_F)/\tau$

Table S3. Optical properties of synthesized compounds in 1wt% polystyrene dispersed film[a]

	$\lambda_{max,abs}$ (nm)[b]	λ_{em} (nm)[c]	Stokes shift (cm^{-1})[d]	Φ_F[e]	τ (ns)[f]	χ^2	k_r ($\times 10^8 s^{-1}$)[g]	k_{nr} ($\times 10^8 s^{-1}$)[g]
monoBAm	412	493	3988	0.013	0.2 (49%) 1.1 (14%) 3.0 (37%)	1.16	0.050	3.8
***syn*-bisBAm**	602	732	2950	0.045	1.7 (53%) 2.7 (47%)	1.08	0.20	4.2
***anti*-bisBAm**	603	737	3015	0.039	2.0 (87%) 5.2 (13%)	1.07	0.14	3.3

[a]Spin-coated film on the quartz substrate (1 cm × 5 cm) prepared from chloroform solution (0.10 mL, 1000 rpm)
[b]The longest absorption maximum
[c]Fluorescence maxima with the excitation at the longest absorption maximum
[d]The difference between the spectral positions of the band maxima of the absorption and emission
[e]Absolute quantum efficiency determined in solid state
[f]Emission lifetime at λ_{em}
[g]$k_r = \Phi_F/\tau_{av}$, $k_{nr} = (1 - \Phi_F)/\tau_{av}$, $\tau_{av} = \Sigma\alpha_i\tau_i^2/\Sigma\alpha_i\tau_i$

Table S4. Optical properties of synthesized compounds in the crystalline states

	λ_{em} (nm)[a]	$\Phi_{F,solid}$[b]	τ (ns)[c]	χ^2	k_r ($\times 10^8 s^{-1}$)[d]	k_{nr} ($\times 10^8 s^{-1}$)[d]
monoBAm	551	0.007	–	–	–	–
***syn*-bisBAm**	757	0.035	0.8 (17%) 1.4 (83%)	1.18	0.27	7.5
***anti*-bisBAm**	745	0.052	1.4 (42%) 2.6 (58%)	1.15	0.23	4.2

[a]Fluorescence maxima with the excitation at the longest absorption maximum determined in solution state
[b]Absolute quantum efficiency determined in solid state
[c]Emission lifetime at λ_{em}
[d]$k_r = \Phi_F/\tau_{av}$, $k_{nr} = (1 - \Phi_F)/\tau_{av}$, $\tau_{av} = \Sigma\alpha_i\tau_i^2/\Sigma\alpha_i\tau_i$

Table S5. Optical properties of synthesized polymers in the spin-coated film[a]

	$\lambda_{max,abs}$ (nm)[b]	λ_{em} (nm)[c]	$\Phi_{F,solid}$[d]
p-bisBAm-F	610	751	0.049
p-bisBAm-T	614	751	0.042

[a]Spin-coated film on the quartz substrate (1 cm × 5 cm) prepared from chloroform solution (0.10 mL, 1000 rpm, concentration: 1.0×10^{-3} M)
[b]The longest absorption maximum
[c]Fluorescence maxima with the excitation at the longest absorption maximum
[d]Absolute quantum efficiency determined in solid state

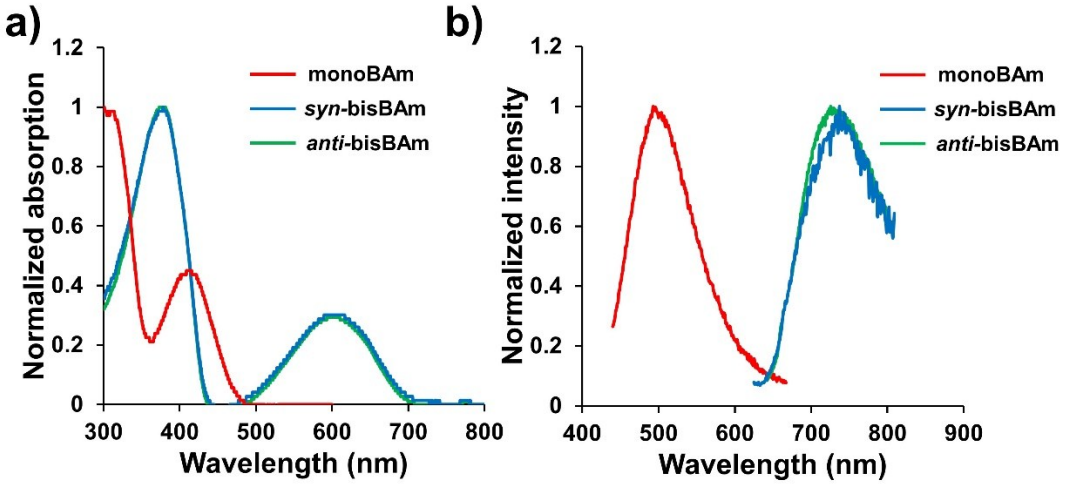

Fig. S29. a) UV–vis absorption b) photoluminescence spectra of 1wt% polystyrene dispersed film of **monoBAm**, ***syn*-bisBAm** and ***anti*-bisBAm**.

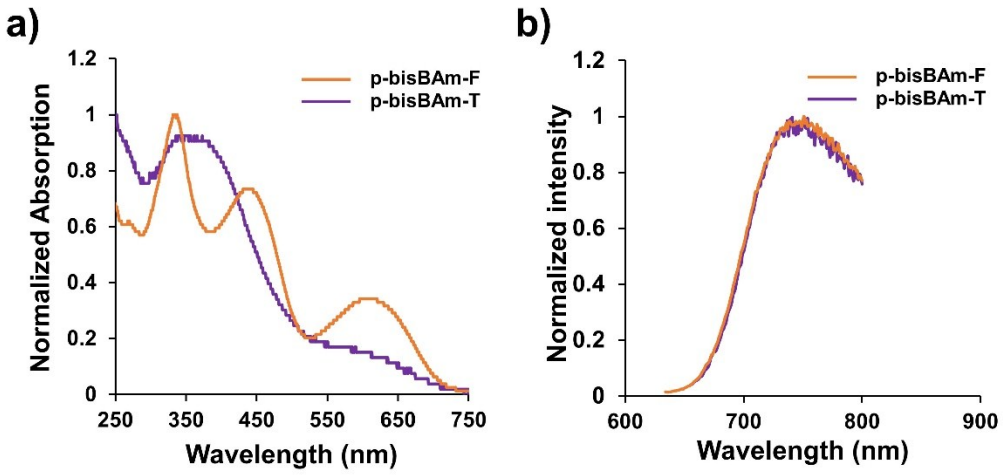

Fig. S30. a) UV–vis absorption and b) photoluminescence spectra of **p-bisBAm-F** (orange solid line) and **p-bisBAm-F** (purple solid line) in spin-coated film.

It was difficult to obtain an emission spectrum above 800 nm region because the sensitivity of the detector (HORIBA Fluorolog-3 luminescence spectrometer) is quite low in this region. We confirmed that the emission spectra showed monotone decreasing above 800 nm region by using Ocean Optics USB4000.

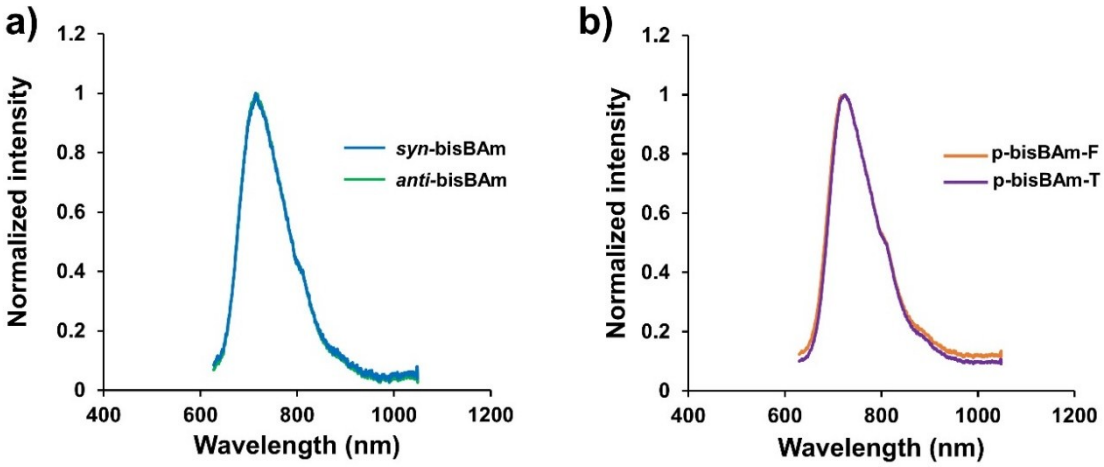

Fig. S31. Photoluminescence spectra of solution state ($CHCl_3$, 1.0×10^{-5} M) obtained by Ocean Optics USB4000 of a) ***syn-*** and ***anti*-bisBAm**, b) **p-bisBAm-F** and **p-bisBAm-T**.

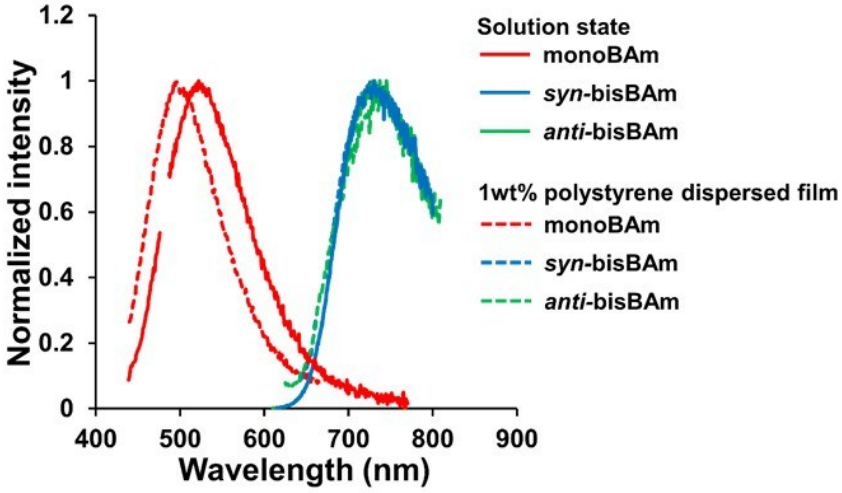

Fig. S32. Photoluminescence spectra of solution state ($CHCl_3$, 1.0×10^{-5} M) and 1wt% polystyrene dispersed film of **monoBAm**, ***syn*-bisBAm** and ***anti*-bisBAm**.

PL life time decay curves

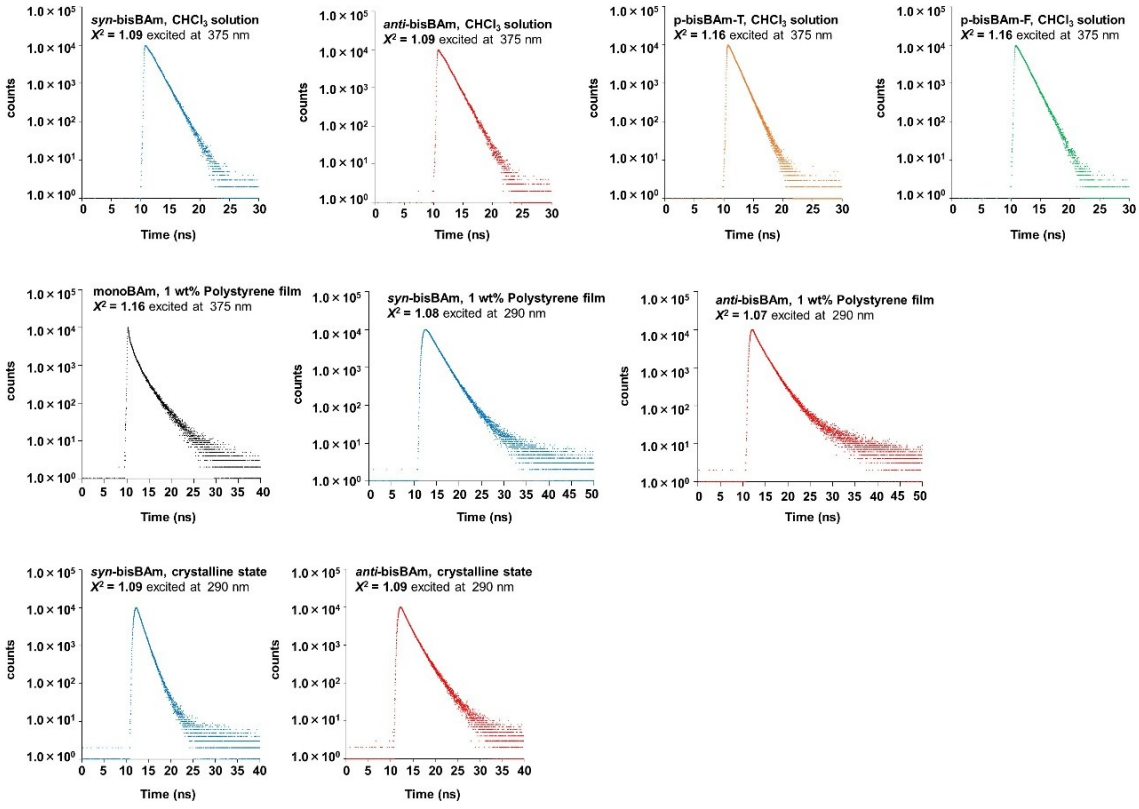

Fig. S33. PL lifetime decay curves of **monoBAm, *syn*-bisBAm *anti*-bisBAm, p-bisBAm-F** and **p-bisBAm-T** in chroloform solution (1.0×10^{-5} M), 1wt% polystyrene film and the crystalline states at room temperature. Their emissions at the PL peak tops were monitored.

Polymerization Results

Table S6. Polymerization results[a]

	Yield (%)[b]	M_n	M_w	M_w/M_n	n[c]
p-bisBAm-F	85	14,400	36,400	2.5	11
p-bisBAm-T	89	11,100	28,300	2.6	8

[a] Estimated by SEC with the polystyrene standards in $CHCl_3$
[b] Isolated yields
[c] Average number of repeating units calculated from M_n and molecular weights of repeating units

Computational Details

The Gaussian 09 program package[2] was used for computation. We optimized the structures of **monoBAmM**, ***syn*-bisBAm**, ***anti*-bisBAm**, **p-bisBAm-F′** and **p-bisBAm-T′** in the ground S_0 states and calculated their molecular orbitals. In **p-bisBAm-F′** and **p-bisBAm-T′**, methyl groups were used as alkyl substituents in place of dodecyl groups of **p-bisBAm-F** and **p-bisBAm-T** for simplification of the calculation. The DFT was applied for the optimization of the structures in the S_0 states at B3LYP/6-311G(d,p) level. We calculated the energy of the S_0–S_1 transitions with optimized geometries in the S_0 states by time-dependent DFT (TD-DFT) at TD-B3LYP/6-311G(d,p) level.

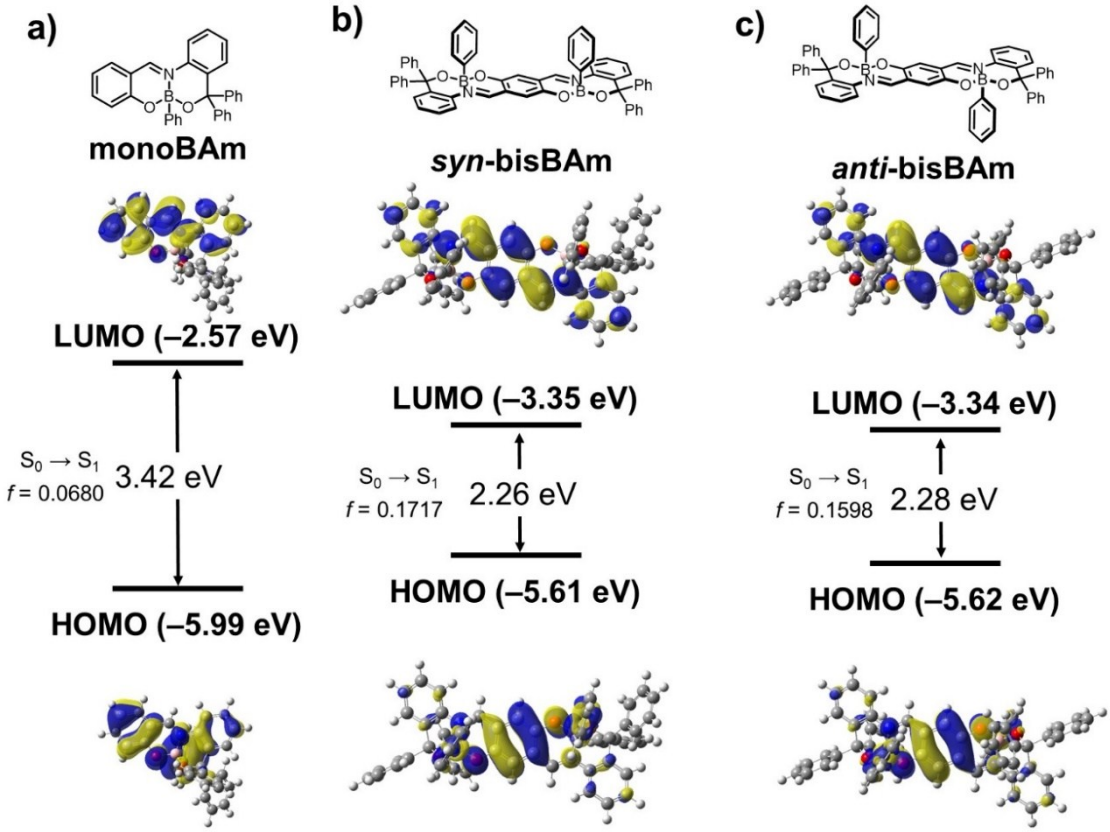

Fig. S34. Structures and molecular orbital diagrams for the LUMO and HOMO of a) **monoBAm** b) ***syn*-bisBAm** c) ***anti*-bisBAm** (B3LYP/6–311G(d,p)//B3LYP/6–311G(d,p)).

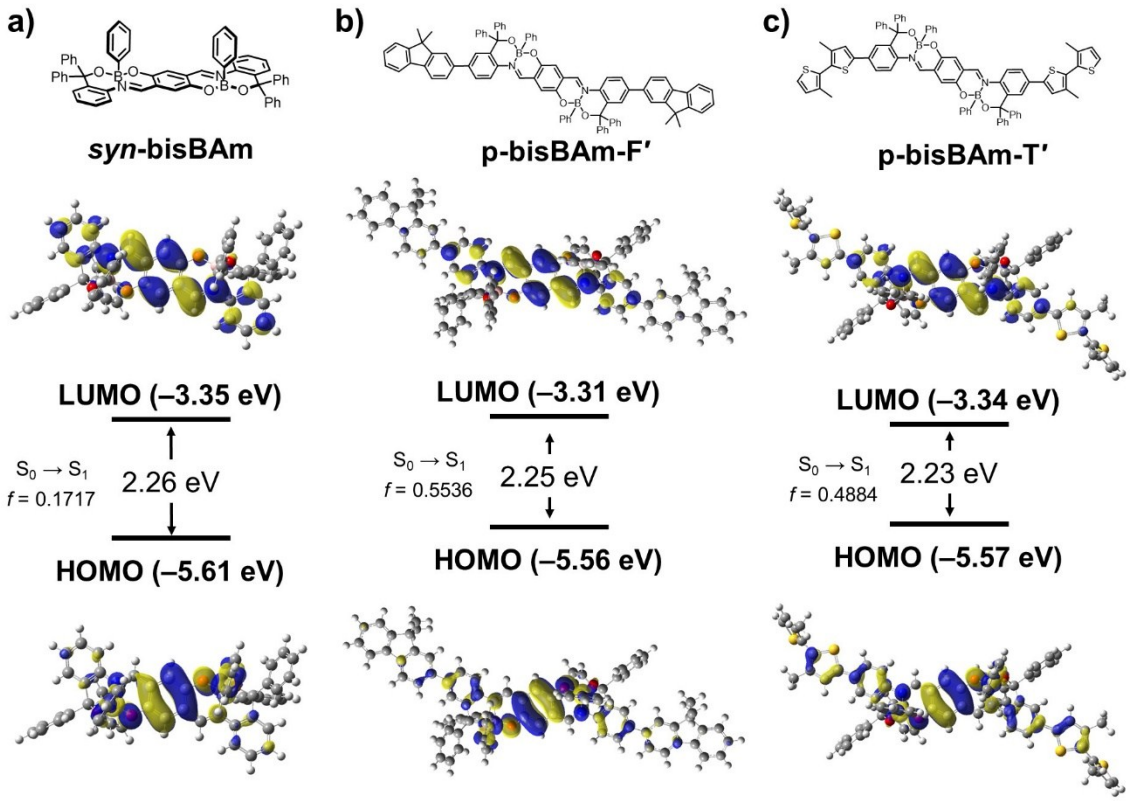

Fig. S35. Structures and molecular orbital diagrams for the LUMO and HOMO of a) **monoBAm** b) **p-bisBAm-F′** c) **p-bisBAm-T′** (B3LYP/6–311G(d,p)//B3LYP/6–311G(d,p)).

Cyclic Voltammograms

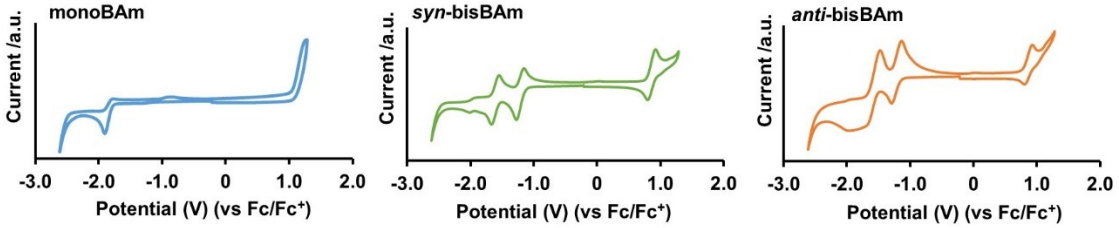

	E_{onset}^{red} /eV	E_{LUMO}[a] /eV	$\Delta E_{g,opt}$[b] /eV	E_{HOMO}[c] /eV
monoBAm	−1.79	−3.01	2.61	−5.62
***syn*-bisBAm**	−1.14	−3.66	1.79	−5.46
***anti*-bisBAm**	−1.15	−3.65	1.80	−5.44

In CH_2Cl_2 (1.0×10^{-3} M), Electrolyte: Bu_4NPF_6 (0.1M)
[a] $E_{LUMO} = -4.8 - E_{onset}^{red}$
[b] Calculated from the onset wavelength of the corresponding UV–vis absorption spectra in $CHCl_3$
[c] $E_{HOMO} = E_{LUMO} - \Delta E_{g,opt}$

Energy diagram

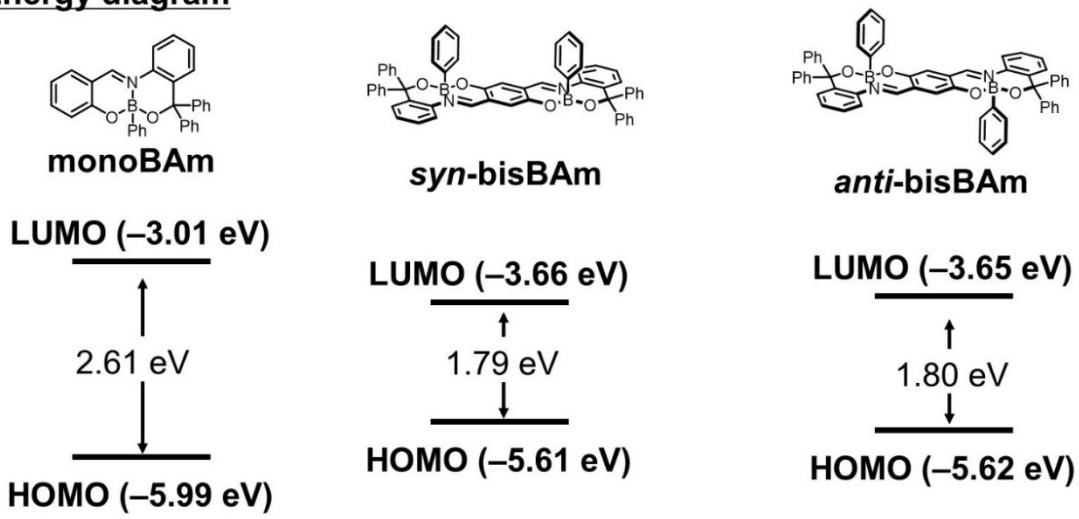

Fig. S36. Cyclic voltammograms of **monoBAm**, ***syn*-bisBAm** and ***anti*-bisBAm** in CH_2Cl_2 (1.0×10^{-3} M, 1.0×10^{-3} M per repeating units for copolymers) containing NBu_4PF_6 (0.10 M) using a glassy carbon (GC) working electrode, a Pt wire counter electrode, an Ag/AgCl reference electrode, and a Fc/Fc^+ external standard at room temperature with a scan rate of 0.1 V s^{-1}.

References

1. Dąbrowski, M.; Kubicka, J.; Luliński, S.; Serwatowski, J. *Tetrahedron* **2005**, *61*, 6590−6595.
2. Gaussian 09, Revision D.01, Frisch, M. J.; Trucks, G. W.; Schlegel, H. B.; Scuseria, G. E.; Robb, M. A.; Cheeseman, J. R.; Scalmani, G.; Barone, V.; Mennucci, B.; Petersson, G. A.; Nakatsuji, H.; Caricato, M.; Li, X.; Hratchian, H. P.; Izmaylov, A. F.; Bloino, J.; Zheng, G.; Sonnenberg, J. L.; Hada, M.; Ehara, M.; Toyota, K.; Fukuda, R.; Hasegawa, J.; Ishida, M.; Nakajima, T.; Honda, Y.; Kitao, O.; Nakai, H.; Vreven, T.; Montgomery, Jr., J. A.; Peralta, J. E.; Ogliaro, F.; Bearpark, M.; Heyd, J. J.; Brothers, E.; Kudin, K. N.; Staroverov, V. N.; Kobayashi, R.; Normand, J.; Raghavachari, K.; Rendell, A.; Burant, J. C. S.; Iyengar, S.; Tomasi, J.; Cossi, M.; Rega, N.; Millam, J. M.; Klene, M.; Knox, J. E.; Cross, J. B.; Bakken, V.; Adamo, C.; Jaramillo, J.; Gomperts, R.; Stratmann, R. E.; Yazyev, O.; Austin, A. J.; Cammi, R.; Pomelli, C.; Ochterski, J. W.; Martin, R. L.; Morokuma, K.; Zakrzewski, V. G.; Voth, G. A.; Salvador, P.; Dannenberg, J. J.; Dapprich, S.; Daniels, A. D.; Farkas, Ö.; Foresman, J. B.; Ortiz, J. V.; Cioslowski, J.; Fox, D. J. Gaussian, Inc., Wallingford CT, 2009.